NASA TECHNICAL NOTE

NASA TN D-4858

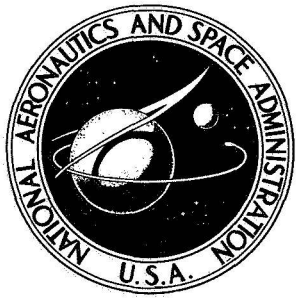

NASA TN D-4858

Corrected Copy

CRITICAL-SPEED ANALYSIS OF RIGID ROTORS ON FLEXIBLE FOUNDATIONS

by Richard H. Cavicchi

Lewis Research Center
Cleveland, Ohio

NATIONAL AERONAUTICS AND SPACE ADMINISTRATION • WASHINGTON, D. C. • JUNE 1969

NASA TN D-4858

CRITICAL-SPEED ANALYSIS OF RIGID ROTORS ON FLEXIBLE FOUNDATIONS

By Richard H. Cavicchi

Lewis Research Center
Cleveland, Ohio

NATIONAL AERONAUTICS AND SPACE ADMINISTRATION

For sale by the Clearinghouse for Federal Scientific and Technical Information
Springfield, Virginia 22151 – CFSTI price $3.00

ABSTRACT

A critical-speed analysis of undamped rigid rotors on flexible foundations reveals four conical-mode solutions comprising forward and backward precession. There is also a two-solution bouncing-mode set dependent only on foundation-to-rotor mass and spring-constant ratios. Although analysis of a firm-foundation model omits two of the four conical-mode solutions, good agreement exists between the two corresponding solutions. The flexible-foundation analysis can be approximated by a simple firm-foundation result when the foundation-to-rotor spring-constant ratio is zero or infinite. Only three calculations are needed in this range to cover all intermediate values.

CRITICAL-SPEED ANALYSIS OF RIGID ROTORS ON FLEXIBLE FOUNDATIONS*

by Richard H. Cavicchi
Lewis Research Center

SUMMARY

A theoretical analysis of rigid rotors in undamped bearings on flexible foundations develops a general frequency equation for both forward and backward precession. One set of two unique solutions comprises the bouncing-mode natural frequency, which is a function of foundation-to-rotor mass and spring-constant ratios, but independent of rotor speed and moments of inertia. Another set, the conical mode, is a function of rotor speed and moments of inertia and contains four unique solutions. Example maps are given for a wide range of rotor speed and of mass, moment-of-inertia ratios, and spring-constant ratios as a guide in preliminary design. Besides locating major critical speeds, the maps locate nonsynchronous critical speeds that may result from bearing defects.

The four conical-mode critical-speed solutions appear on the maps as a high- and low-frequency set of two-branch curves. Although the firm-foundation analysis omits two of these critical speeds, its two existing solutions agree well with flexible-foundation results. Furthermore, the two omitted critical speeds can be approximated by the two firm-foundation bouncing-mode solutions. The flexible-foundation analysis can be approximated by the two-solution firm-foundation result for the zero and infinite extremities of the foundation-to-rotor spring-constant ratio. Therefore, only three flexible-foundation calculations are needed within this range to cover all intermediate values.

INTRODUCTION

Stationary turbomachinery is customarily mounted on rigid foundations. Therefore, many theoretical studies of rotor vibration assume firm foundations, as in reference 1. An important extension is to regard the foundation itself as flexibly supported. Such configurations are more representative of aircraft and spacecraft installations. Analysis of models for this application is complicated by the addition of at least two variables to those of firm-foundation models.

---

*The original version of this report has been corrected to use gyroscopic terms based on the rotor absolute angle instead of on the relative angle between the rotor and foundation.

Crook and Grantham report in reference 2 on a method of predicting synchronous vibrations of rotors on underdamped flexible foundations. By including the energy loss associated with damping factors checked by experiment, they show close agreement between theory and observation. Gunter's work on a flexible-foundation analysis in reference 3 reveals that proper foundation design can provide considerable improvement in rotor stability characteristics.

The present report extends the methods of reference 1 to include vibratory motion of the foundation. It derives the general frequency equation, presents the results of a parametric analysis of rotor dynamic frequencies and critical speeds, and gives some selected examples. The purpose of this report is to aid in preliminary design of turbomachinery by providing guidance to the location of potential synchronous and nonsynchronous critical speeds.

The work presented here covers a wide range of rotor shapes, rotor speeds, and foundation shapes. The centers of gravity of the rotor and foundation in the present model remain fixed midway between the bearings. Damping and unbalance forces are neglected in this analysis to isolate the effects of shape, speed, and spring-constant variations.

SYMBOLS

A, B, C, D, E, F, G, H	vibration amplitude, m
a_1, a_2, a_3, a_4	constant functions of π_3, π_5, and π_6
I	polar moment-of-inertia of rotor, kg-m^2
I_1	diametral moment-of-inertia of rotor, kg-m^2
I_1'	moment of inertia of foundation, kg-m^2
$k_1/2$	linear spring constant of rotor bearings, kg/sec^2
$k_2/2$	linear spring constant of foundation, kg/sec^2
l	distance between bearings, and also between foundation mounts, m
M	rotor mass, kg
M'	foundation mass, kg
p	rotor precession frequency, rad/sec
r	critical-speed ratio, $r = \pi_1/\pi_4 = p/\omega$
S	square of rotor frequency parameter, $\pi_1^2 = \left(p/\sqrt{k_1/M}\right)^2$
t	time, sec

y_1, y_2 lateral distance from arbitrary reference frame to rotor bearings, m

y'_1, y'_2 lateral distance from arbitrary reference frame to foundation mounts, m

$z_1 z_2$ lateral distance from arbitrary reference frame to rotor bearings (perpendicular to y_1 and y_2), m

$z'_1 z'_2$ lateral distance from arbitrary reference frame to foundation mounts (perpendicular to y'_1 and y'_2), m

π_1 frequency parameter, $p/\sqrt{k_1/M} = \sqrt{S}$

π_2 rotor disk effect, I_1/Ml^2

π_3 rotor polar-to-diametral moment-of-inertia ratio, I/I_1

π_4 rotor rotational-speed parameter, $\omega/\sqrt{k_1/M}$

π_5 foundation-to-rotor moment-of-inertia ratio, I'_1/I_1

π_6 foundation-to-rotor spring-constant ratio, k_2/k_1

π_7 foundation-to-rotor mass ratio, M'/M

ω rotor rotational speed, rad/sec

Subscript:

cr major critical

Superscripts:

$\dot{}$ first derivative with respect to time

$\ddot{}$ second derivative with respect to time

DESCRIPTION OF ROTOR-FOUNDATION MODEL

Figure 1 is a schematic representation of a rigid rotor with flexible bearings on pedestals attached to a flexible foundation. This study considers motions in the lateral mutually perpendicular directions y, y' and z, z' directions. Consideration of axial motion is excluded.

No damping or unbalance forces are assumed in the model of figure 1. The centers of gravity of the rotor and foundation masses are assumed to be midway between the rotor bearings. All bearings are assumed to be linear springs. In both lateral directions the rotor-bearing spring constant is $k_1/2$ and that of the foundation is $k_2/2$ (see fig. 1).

To this extent, there is one less variable in the present analysis than in that of reference 1, because the center-of-gravity location is fixed. An additional variable is

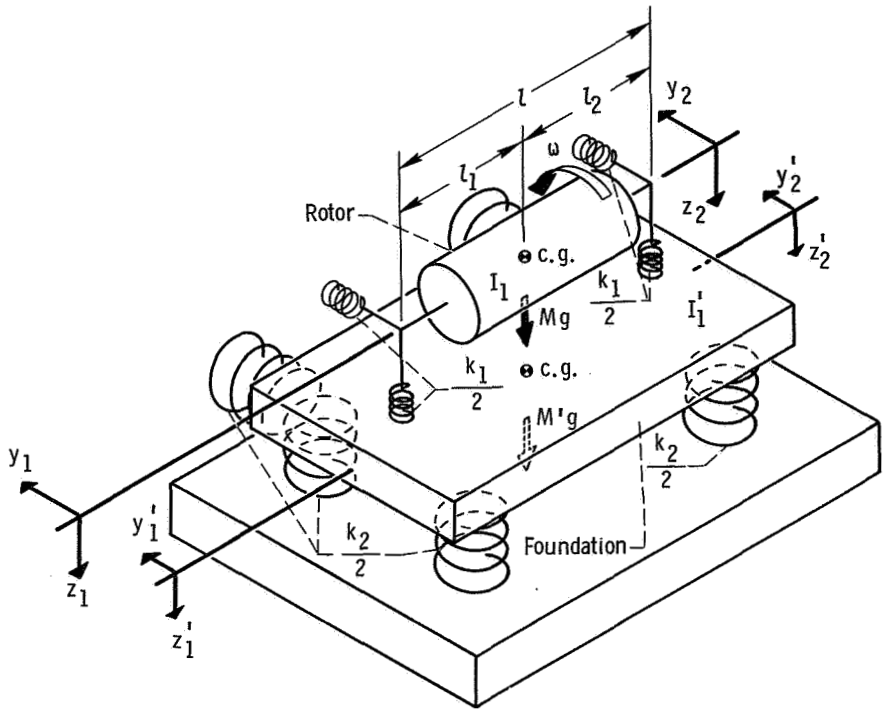

Figure 1. - Schematic sketch of a rigid rotor on a flexible foundation.

added, however, due to foundation flexibility in terms of the spring constant k_2. Furthermore, the presence of the vibrating foundation mass adds two more variables - its mass M' and moment of inertia I_1'. The net result is that the present analysis is complicated by two more variables than that of reference 1.

Rotor slenderness ratio is introduced into the mathematical analysis in terms of the rotor polar moment of inertia I and the diametral moment of inertia I_1. The rotor moments of inertia are expressed as the following nondimensional parameters:

Rotor disk effect:

$$\pi_2 = \frac{I_1}{Ml^2} \tag{1}$$

Rotor polar-to-diametral moment-of-inertia ratio:

$$\pi_3 = \frac{I}{I_1} \tag{2}$$

The parameters π_2 and π_3 are small for pencil shapes, and larger for disks. The parameter π_2 is the disk effect used in reference 4. For a concentrated mass, $\pi_2 = 0$,

and for a disk having all its mass distributed over a large radius, $\pi_2 = \infty$. The ratio $\pi_3 = 0.0149$ for a rod whose length is 10 times its diameter. For a disk of negligible thickness, $\pi_3 = 2$. Therefore, configurations become more like disks as π_2 and π_3 increase.

ANALYSIS

This section presents the equations of motion for the simplified model shown in figure 1. Solution of the equations of motion leads to a general frequency equation. This equation is applied to various special conditions of geometry and speed to cover the wide range of conditions used in the examples.

The object of this analysis is to study the frequency and critical-speed characteristics of the model in figure 1. Therefore, no attempt is made to solve the equations for vibration amplitudes.

Equations of Motion

Derivation of the following equations of motion was motivated by the work of Timoshenko in reference 5. The equations include the assumption of small rotor and foundation displacements:

Rotor:

$$M\ddot{y}_1 + M\ddot{y}_2 + k_1(y_1 - y_1') + k_1(y_2 - y_2') = 0 \tag{3}$$

$$M\ddot{z}_1 + M\ddot{z}_2 + k_1(z_1 - z_1') + k_1(z_2 - z_2') = 0 \tag{4}$$

$$I\omega(\dot{y}_2 - \dot{y}_1) - I_1(\ddot{z}_2 - \ddot{z}_1) - \frac{k_1 l^2}{4}(z_2 - z_2') + \frac{k_1 l^2}{4}(z_1 - z_1') = 0 \tag{5}$$

$$I\omega(\dot{z}_2 - \dot{z}_1) + I_1(\ddot{y}_2 - \ddot{y}_1) + \frac{k_1 l^2}{4}(y_2 - y_2') - \frac{k_1 l^2}{4}(y_1 - y_1') = 0 \tag{6}$$

Foundation:

$$M'\ddot{y}_1' + M'\ddot{y}_2' - k_1(y_1 + y_2) + (k_1 + k_2)(y_1' + y_2') = 0 \tag{7}$$

$$M'\ddot{z}'_1 + M'\ddot{z}'_2 - k_1(z_1 + z_2) + (k_1 + k_2)(z'_1 + z'_2) = 0 \tag{8}$$

$$-I'_1(\ddot{z}'_2 - \ddot{z}'_1) + \frac{(k_1 + k_2)l^2}{4}(z'_1 - z'_2) - \frac{k_1 l^2}{4}(z_1 - z_2) = 0 \tag{9}$$

$$I'_1(\ddot{y}'_2 - \ddot{y}'_1) - \frac{(k_1 + k_2)l^2}{4}(y'_1 - y'_2) + \frac{k_1 l^2}{4}(y_1 - y_2) = 0 \tag{10}$$

Frequency Solutions

Assumed solutions. - Den Hartog (ref. 4) solves problems of two masses joined by springs by assuming that both masses execute harmonic motions with the same frequency. This assumption is conservative, because it represents a resonant condition in which the motions of the two masses reinforce each other. This is the most critical condition, and is the one to be avoided if possible.

Accordingly, the same frequency p appears in all of the following assumed solutions:

$$y_1 = A \sin pt \tag{11}$$

$$y_2 = B \sin pt \tag{12}$$

$$z_1 = C \cos pt \tag{13}$$

$$z_2 = D \cos pt \tag{14}$$

$$y'_1 = E \sin pt \tag{15}$$

$$y'_2 = F \sin pt \tag{16}$$

$$z'_1 = G \cos pt \tag{17}$$

$$z'_2 = H \cos pt \tag{18}$$

Coefficient matrix. - When equations (11) to (18) are inserted into equations (3) to (10), the following set results:

$$A(k_1 - Mp^2) + B(k_1 - Mp^2) - Ek_1 - Fk_1 = 0 \tag{19}$$

$$C(k_1 - Mp^2) + D(k_1 - Mp^2) - Gk_1 - Hk_1 = 0 \tag{20}$$

$$-A(I\omega p) + B(I\omega p) + C\left(\frac{k_1 l^2}{4} - I_1 p^2\right) - D\left(\frac{k_1 l^2}{4} - I_1 p^2\right) - G\left(\frac{k_1 l^2}{4}\right) + H\left(\frac{k_1 l^2}{4}\right) = 0 \tag{21}$$

$$-A\left(\frac{k_1 l^2}{4} - I_1 p^2\right) + B\left(\frac{k_1 l^2}{4} - I_1 p^2\right) + C(I\omega p) - D(I\omega p) + E\left(\frac{k_1 l^2}{4}\right) - F\left(\frac{k_1 l^2}{4}\right) = 0 \tag{22}$$

$$-Ak_1 - Bk_1 + E\left[(k_1 + k_2) - M'p^2\right] + F\left[(k_1 + k_2) - M'p^2\right] = 0 \tag{23}$$

$$-Ck_1 - Dk_1 + G\left[(k_1 + k_2) - M'p^2\right] + H\left[(k_1 + k_2) - M'p^2\right] = 0 \tag{24}$$

$$-C\left(\frac{k_1 l^2}{4}\right) + D\left(\frac{k_1 l^2}{4}\right) + G\left[\frac{(k_1 + k_2) l^2}{4} - I_1' p^2\right] - H\left[\frac{(k_1 + k_2) l^2}{4} - I_1' p^2\right] = 0 \tag{25}$$

$$A\left(\frac{k_1 l^2}{4}\right) - B\left(\frac{k_1 l^2}{4}\right) - E\left[\frac{(k_1 + k_2) l^2}{4} - I_1' p^2\right] + F\left[\frac{(k_1 + k_2) l^2}{4} - I_1' p^2\right] = 0 \tag{26}$$

In matrix form, this set is

$$\begin{bmatrix}
(k_1 - Mp^2) & (k_1 - Mp^2) & 0 & 0 & -k_1 & -k_1 & 0 & 0 \\
0 & 0 & (k_1 - Mp^2) & (k_1 - Mp^2) & 0 & 0 & -k_1 & -k_1 \\
-I\omega p & I\omega p & \left(\frac{k_1 l^2}{4} - I_1 p^2\right) & -\left(\frac{k_1 l^2}{4} - I_1 p^2\right) & 0 & 0 & -\frac{k_1 l^2}{4} & \frac{k_1 l^2}{4} \\
-\left(\frac{k_1 l^2}{4} - I_1 p^2\right) & \left(\frac{k_1 l^2}{4} - I_1 p^2\right) & I\omega p & -I\omega p & \frac{k_1 l^2}{4} & -\frac{k_1 l^2}{4} & 0 & 0 \\
-k_1 & -k_1 & 0 & 0 & \left[(k_1 + k_2) - M'p^2\right] & \left[(k_1 + k_2) - M'p^2\right] & 0 & 0 \\
0 & 0 & -k_1 & -k_1 & 0 & 0 & \left[(k_1 + k_2) - M'p^2\right] & \left[(k_1 + k_2) - M'p^2\right] \\
0 & 0 & -\frac{k_1 l^2}{4} & \frac{k_1 l^2}{4} & 0 & 0 & \left[\frac{(k_1 + k_2) l^2}{4} - I'_1 p^2\right] & -\left[\frac{(k_1 + k_2) l^2}{4} - I'_1 p^2\right] \\
\frac{k_1 l^2}{4} & -\frac{k_1 l^2}{4} & 0 & 0 & -\left[\frac{(k_1 + k_2) l^2}{4} - I'_1 p^2\right] & \left[\frac{(k_1 + k_2) l^2}{4} - I'_1 p^2\right] & 0 & 0
\end{bmatrix}
\begin{Bmatrix} A \\ B \\ C \\ D \\ E \\ F \\ G \\ H \end{Bmatrix} = 0 \qquad (27)$$

Determinant reduction. - Nontrivial solutions of A, B, C, D, E, F, G, and H in equations (19) to (26) require that the determinant of the coefficient matrix given in equation (27) vanish. Reduction of this determinant leads to the general frequency equation

$$\left\{(k_1 - Mp^2)\left[(k_1 + k_2) - M'p^2\right] - k_1^2\right\}^2 \begin{vmatrix}
-I\omega p & \left(\frac{k_1 l^2}{4} - I_1 p^2\right) & 0 & -\frac{k_1 l^2}{4} \\
-\left(\frac{k_1 l^2}{4} - I_1 p^2\right) & I\omega p & \frac{k_1 l^2}{4} & 0 \\
0 & -\frac{k_1 l^2}{4} & 0 & \left[\frac{(k_1 + k_2) l^2}{4} - I'_1 p^2\right] \\
\frac{k_1 l^2}{4} & 0 & -\left[\frac{(k_1 + k_2) l^2}{4} - I'_1 p^2\right] & 0
\end{vmatrix} = 0 \qquad (28)$$

Equation (28) is of the 16^{th} order in p. There must therefore be 16 solutions, although not all are unique. In equation (28), the determinant and its multiplying factor each contains eight solutions.

Nondimensional parameters. - Expressing the variables in equation (28) in nondi-

mensional form is especially helpful in solving the equation and presenting the results. The nondimensional parameters and their nomenclatures are defined as follows:

Precession frequency parameter:

$$\pi_1 = \frac{p}{\sqrt{k_1/M}} \tag{29}$$

Rotor disk effect:

$$\pi_2 = \frac{I_1}{M\ell^2} \tag{1}$$

Rotor polar-to-diametral moment-of-inertia ratio:

$$\pi_3 = \frac{I}{I_1} \tag{2}$$

Rotor-rotational-speed parameter:

$$\pi_4 = \frac{\omega}{\sqrt{k_1/M}} \tag{30}$$

Foundation-to-rotor moment-of-inertia ratio:

$$\pi_5 = \frac{I_1'}{I_1} \tag{31}$$

Foundation-to-rotor spring-constant ratio:

$$\pi_6 = \frac{k_2}{k_1} \tag{32}$$

Foundation-to-rotor mass ratio:

$$\pi_7 = \frac{M'}{M} \tag{33}$$

An objective of this analysis henceforth will be to identify frequency solutions for π_1 instead of p. It will be seen that definition of another parameter S simplifies the appearance of high-degree polynomials by halving their orders:

$$S = \pi_1^2 = \left(\frac{p}{\sqrt{k_1/M}}\right)^2 \tag{34}$$

Nondimensional general frequency equation. - With the use of the nondimensional parameters defined by equations (1), (2), and (29) to (33), the general frequency equation (eq. (28)) assumes the following nondimensional form:

$$\left\{\left(1 - \pi_1^2\right)\left[(1 + \pi_6) - \pi_7\pi_1^2\right] - 1\right\}^2 \begin{vmatrix} -\pi_1\pi_3\pi_4 & \left(\frac{1}{4\pi_2} - \pi_1^2\right) & 0 & -\frac{1}{4\pi_2} \\ -\left(\frac{1}{4\pi_2} - \pi_1^2\right) & \pi_1\pi_3\pi_4 & \frac{1}{4\pi_2} & 0 \\ 0 & -\frac{1}{4\pi_2} & 0 & \left(\frac{1 + \pi_6}{4\pi_2} - \pi_1^2\pi_5\right) \\ \frac{1}{4\pi_2} & 0 & -\left(\frac{1 + \pi_6}{4\pi_2} - \pi_1^2\pi_5\right) & 0 \end{vmatrix} = 0 \tag{35}$$

Mode Frequency Equations

In equation (35), both the determinant and its multiplying factor contain valid solutions. Solutions for π_1 obtained from this factor represent the bouncing-mode natural frequency. The rotor rotational-speed parameter π_4 and moment-of-inertia ratios π_2, π_3, and π_5 do not appear in this factor. Therefore, the bouncing mode solutions are the natural frequencies that exist whether the rotor is rotating or not.

The determinant in equation (35) yields the conical-mode solutions, which are functions of rotor speed and the moment-of-inertia ratios. The foundation-to-rotor mass

ratio π_7, however, is absent from the determinant. Masses M and M' exist in the determinant, of course, in terms of the moment-of-inertia ratios. The conical mode consists of the rotor precessions performed as the rotor axis describes the surface of an imaginary cone. The study of the conical-mode solutions is a primary concern of this analysis.

Bouncing mode. - Equating to zero the factor outside the determinant in equation (35) and using equation (34) yield the bouncing-mode frequency equation

$$\left(\frac{\pi_7}{\pi_6}\right)S^2 - \left(1 + \frac{1}{\pi_6} + \frac{\pi_7}{\pi_6}\right)S + 1 = 0 \tag{36}$$

The solution of this quadratic expression is

$$S = \frac{\pi_6}{2\pi_7}\left[\left(1 + \frac{1}{\pi_6} + \frac{\pi_7}{\pi_6}\right) \pm \sqrt{\left(1 + \frac{1}{\pi_6} + \frac{\pi_7}{\pi_6}\right)^2 - \frac{4\pi_7}{\pi_6}}\right] \tag{37}$$

Values of S greater than one result from using the positive sign in this expression. The negative sign yields values of S less than or equal to one.

Equation (37), by way of equation (34), represents 4 of the total of 16 solutions for p or π_1 contained in equations (28) or (35). Because the factor outside the determinant in equation (35) is of second degree, there exists a duplicate set of the four solutions for π_1 contained in equation (37). Of these eight solutions, only two are unique.

Conical mode. - The conical-mode frequency equation is obtained by equating the determinant in equation (35) to zero. The result is

$$\left(\frac{\pi_2\pi_5}{\pi_6}\right)^2 S^4 - \frac{\pi_2\pi_5}{\pi_6}\left[\left(\frac{\pi_2\pi_5}{\pi_6}\right)\pi_3^2\pi_4^2 + \frac{1}{2} + \frac{\pi_5}{2\pi_6} + \frac{1}{2\pi_6}\right]S^3$$

$$+ \frac{1}{2}\left[\left(\frac{\pi_2\pi_5}{\pi_6}\right)\pi_3^2\pi_4^2\left(1 + \frac{1}{\pi_6}\right) + \frac{\pi_5^2}{8\pi_6^2} + \frac{\pi_5}{2\pi_6} + \frac{1}{4\pi_6} + \frac{\pi_5}{4\pi_6^2} + \frac{1}{8} + \frac{1}{8\pi_6^2}\right]S^2$$

$$- \frac{1}{16}\left[\pi_3^2\pi_4^2\left(1 + \frac{1}{\pi_6}\right) + \frac{1}{2\pi_2\pi_6} + \frac{\pi_5}{2\pi_2\pi_6} + \frac{1}{2\pi_2}\right]S + \frac{1}{256\pi_2^2} = 0 \tag{38}$$

Solving this quartic equation for S is cumbersome. It is more convenient to solve equation (38) for the shape-speed parameter $\pi_3\pi_4$. The resulting expression is

$$\pi_3\pi_4 = \frac{1}{\sqrt{S}}\left[\frac{1}{\frac{\pi_2\pi_5 S}{\pi_6} - \frac{\left(1+\frac{1}{\pi_6}\right)}{4}}\right]\left\{\left(\frac{\pi_2\pi_5}{\pi_6}\right)^2 S^4 - \left(\frac{\pi_2\pi_5}{2\pi_6}\right)\left(1+\frac{\pi_5}{\pi_6}+\frac{1}{\pi_6}\right)S^3\right.$$

$$\left. + \left[\frac{1}{2\pi_6^2}\left(\frac{1}{2}+\pi_5+\frac{\pi_5^2}{2}\right)+\frac{1}{\pi_6}\left(\frac{1}{2}+\pi_5\right)+\frac{1}{4}\right]\frac{S^2}{4} - \left(\frac{1}{32\pi_2}\right)\left(1+\frac{\pi_5}{\pi_6}+\frac{1}{\pi_6}\right)S + \left(\frac{1}{16\pi_2}\right)^2\right\}^{1/2} \qquad (39)$$

Further simplification is possible by multiplying equation (39) by $\sqrt{\pi_2}$ and considering $(S\pi_2)$ and $\left(\pi_4\sqrt{\pi_2}\right)$ as the variables. Therefore, equation (39) becomes

$$\pi_3\left(\pi_4\sqrt{\pi_2}\right) = \frac{1}{\sqrt{S\pi_2}}\left[\frac{1}{\left(\frac{\pi_5}{\pi_6}\right)(S\pi_2) - \frac{\left(1+\frac{1}{\pi_6}\right)}{4}}\right]\left\{\left(\frac{\pi_5}{\pi_6}\right)^2 (S\pi_2)^4 - \left(\frac{\pi_5}{2\pi_6}\right)\left(1+\frac{\pi_5}{\pi_6}+\frac{1}{\pi_6}\right)(S\pi_2)^3\right.$$

$$\left. + \frac{1}{4}\left[\frac{1}{4\pi_6^2}(1+\pi_5)^2+\frac{1}{\pi_6}\left(\frac{1}{2}+\pi_5\right)+\frac{1}{4}\right](S\pi_2)^2 - \frac{1}{32}\left(1+\frac{\pi_5}{\pi_6}+\frac{1}{\pi_6}\right)(S\pi_2)+\left(\frac{1}{16}\right)^2\right\}^{1/2} \qquad (40)$$

The arrangement $(S\pi_2)$ in effect reduces the number of variables by 1.

As $(S\pi_2) \to 0$ in equation (40), the relation

$$\left[\pi_3\left(\pi_4\sqrt{\pi_2}\right)\right]\left(\pi_1\sqrt{\pi_2}\right) = -\frac{1}{4}\left(\frac{1}{1+\frac{1}{\pi_6}}\right) \tag{41}$$

exists with the aid of equation (34). This relation is approached asymptotically by backward precession in the low-frequency set.

As $(S\pi_2) \to \infty$ and $\left(\pi_4\sqrt{\pi_2}\right) \to \infty$ in equation (40), the ratio

$$\frac{\pi_1\sqrt{\pi_2}}{\pi_3\left(\pi_4\sqrt{\pi_2}\right)} = 1 \tag{42}$$

is approached for all shapes, irrespective of π_5 and π_6. The relation expressed by equation (42) applies to the condition of forward precession in the high-frequency set.

When the spring-constant ratio $\pi_6 \to 0$, an approximate form of equation (40) is

$$\pi_3^2\left(\pi_4^2\pi_2\right)(S\pi_2) = (S\pi_2)^2 - \frac{S\pi_2}{2}\left(1+\frac{1}{\pi_5}\right) + \frac{1}{16}\left(1+\frac{1}{\pi_5}\right)^2 \tag{43}$$

To provide physical significance of the zero condition for π_6, it may be considered that it is approached by rotors in aircraft or spacecraft (floating foundation). Very hard spring rotor-bearing mounts also approach this condition.

A remarkable simplification to the solution of equation (43) is available by noting that the right side is a perfect square. A convenient form is

$$\delta\pi_3\frac{2\left(\pi_4\sqrt{\pi_2}\right)}{\sqrt{1+\frac{1}{\pi_5}}} = \frac{2\pi_1\sqrt{\pi_2}}{\sqrt{1+\frac{1}{\pi_5}}} - \frac{1}{\frac{2\pi_1\sqrt{\pi_2}}{\sqrt{1+\frac{1}{\pi_5}}}} \tag{44}$$

where

$$\left.\begin{aligned}\delta &= 1 \quad \text{for forward precession}\\ \text{and}\\ \delta &= -1 \quad \text{for backward precession}\end{aligned}\right\} \tag{45}$$

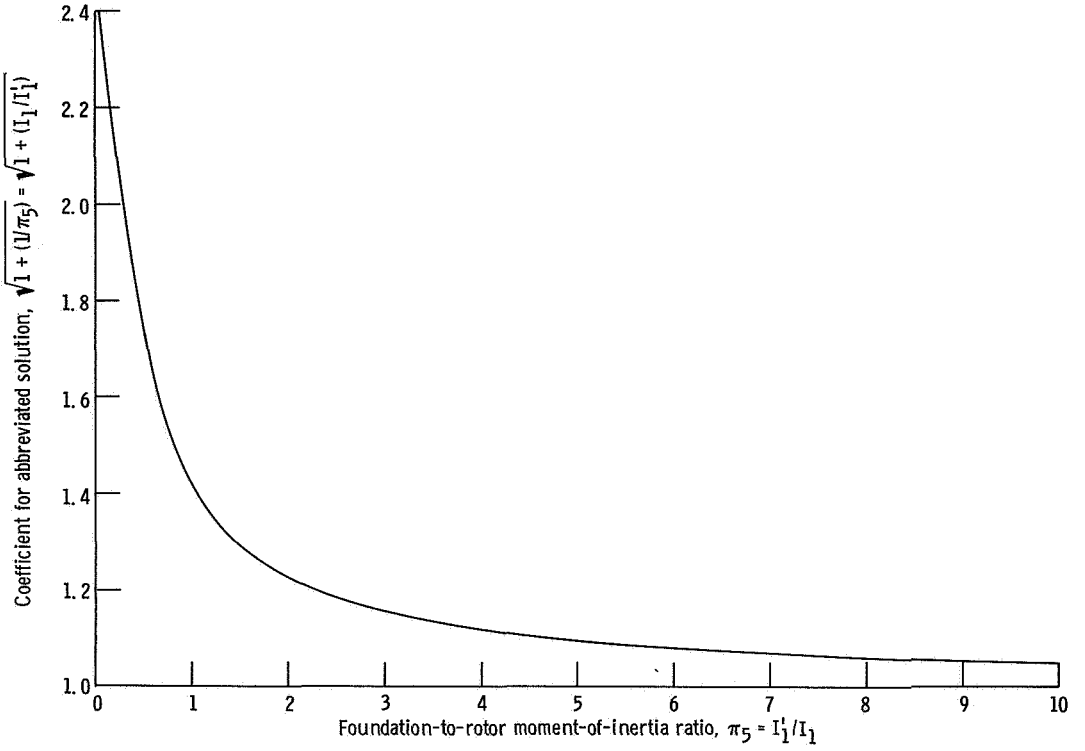

Figure 2. - Coefficient for abbreviated solution (for use in eq. (44)).

The technique of displaying the frequency equation in the form of equation (44) was suggested by Den Hartog in reference 4. It was also used in reference 1.

Figure 2 presents the variation with the foundation-to-rotor moment-of-inertia ratio π_5 of the coefficient $\sqrt{1 + (1/\pi_5)}$ in equation (44). The sensitivity becomes extreme when $\pi_5 < 1$, which represents a large rotor on a small foundation.

When the spring-constant ratio π_6 and square of the adjusted frequency parameter $S\pi_2$ both become large (high-frequency set), equation (40) reduces to the relation

$$S\pi_2 = \frac{\pi_6}{4\pi_5} \tag{46}$$

or

$$\pi_1 \sqrt{\pi_2} = \frac{1}{2} \sqrt{\frac{\pi_6}{\pi_5}} \tag{47}$$

which is a parabola in $\pi_1\sqrt{\pi_2}$ and π_6. A large value of π_6 approaches the condition for a firm foundation. This condition also applies to very soft rotor-bearing mounts on a flexible or firm foundation. The expression in equation (47), which will be discussed on page 29 in connection with figure 7, applies to the high-frequency set of solutions. Equations (46) and (47) also result from equation (40) when the adjusted shape-speed parameter $\pi_3\left(\pi_4\sqrt{\pi_2}\right)$ becomes large, as by high rotor rotational speed.

When π_6 becomes large with $S\pi_2$ remaining finite (low-frequency set), equation (40) becomes

$$\pi_3^2\left(\pi_4^2\pi_2\right)(S\pi_2) = (S\pi_2)^2 - \frac{S\pi_2}{2} + \frac{1}{16} \tag{48}$$

It is interesting to note that equation (43) reduces to the expression in equation (48) as $\pi_5 \to \infty$. This condition pertains to small rotors on large foundations.

Again, because of the perfect square on the right side of equation (48), its solution is

$$\delta\pi_3 2\left(\pi_4\sqrt{\pi_2}\right) = 2\left(\pi_1\sqrt{\pi_2}\right) - \frac{1}{2\left(\pi_1\sqrt{\pi_2}\right)} \tag{49}$$

This result is identical to that reported in reference 1 for the case with the center of gravity midway between the bearings.

At zero rotor rotational speed, equation (44) reduces to

$$\pi_1\sqrt{\pi_2} = \frac{1}{2}\sqrt{1 + \frac{1}{\pi_5}} \tag{50}$$

and equation (49) becomes

$$\pi_1\sqrt{\pi_2} = \frac{1}{2} \tag{51}$$

These solutions are entirely apart from the bouncing-mode frequencies of equation (37) because of the fundamental difference in their derivations. Certain geometrical conditions do exist, of course, in which the frequencies of the two modes could coincide. The result of equating expressions for S obtained from equations (37) and (50) is

$$\frac{1+\frac{1}{\pi_5}}{4\pi_2} = \frac{\pi_6}{2\pi_7}\left[\left(1+\frac{1}{\pi_6}+\frac{\pi_7}{\pi_6}\right) \pm \sqrt{\left(1+\frac{1}{\pi_6}+\frac{\pi_7}{\pi_6}\right)^2 - \frac{4\pi_7}{\pi_6}}\right] \tag{52}$$

Forcing the zero-speed and bouncing-mode frequencies to be equal in this way is primarily an artificial procedure. It is hoped that pointing out the artificiality will help avoid confusion between the zero-speed and bouncing-mode frequencies.

Critical Speeds

A critical speed is defined as any rotor rotational speed at which vibration amplification occurs. The bouncing mode is excluded from this classification because it is independent of rotor speed. The critical-speed ratio is

$$r = \frac{\pi_1}{\pi_4} = \frac{p}{\omega} \tag{53}$$

When this relation together with equation (34) is used in equation (40), the following fourth-order equation in $S\pi_2$ results:

$$256\left(\frac{\pi_5}{\pi_6}\right)^2\left(\frac{\pi_3^2}{r^2}-1\right)(S\pi_2)^4 - 128\left(\frac{\pi_5}{\pi_6}\right)\left[\frac{\pi_3^2}{r^2}\left(1+\frac{1}{\pi_6}\right) - 1 - \frac{\pi_5}{\pi_6} - \frac{1}{\pi_6}\right](S\pi_2)^3$$

$$+ 16\left[\frac{\pi_3^2}{r^2}\left(1+\frac{1}{\pi_6}\right)^2 - 1 - \frac{4\pi_5}{\pi_6} - \frac{2\pi_5}{\pi_6^2} - \frac{\pi_5^2}{\pi_6^2} - \frac{2}{\pi_6} - \frac{1}{\pi_6^2}\right](S\pi_2)^2$$

$$+ 8\left(1+\frac{\pi_5}{\pi_6}+\frac{1}{\pi_6}\right)(S\pi_2) - 1 = 0 \tag{54}$$

A concise form of this expression is

$$a_4(S\pi_2)^4 + a_3(S\pi_2)^3 + a_2(S\pi_2)^2 + a_1(S\pi_2) - 1 = 0 \tag{55}$$

When a_1, a_2, a_3, and a_4 are constant, equation (55) yields four solutions of the type

$$S\pi_2 = K^2 \tag{56}$$

or

$$\pi_1 \sqrt{\pi_2} = K \tag{57}$$

The eight roots given by equation (57) are all real when $\pi_3/r < 1$, as equation (54) shows. Six roots are real and there is a complex conjugate pair when $\pi_3/r \geq 1$. The six real roots comprise two sets of mirror images.

The mathematical condition for major critical speed is obtained from equation (53) by setting

$$r = \frac{\pi_1}{\pi_4} = 1 \tag{58}$$

When this relation is used in equation (54), the result is

$$256\left(\frac{\pi_5}{\pi_6}\right)^2\left(\pi_3^2 - 1\right)(S\pi_2)^4 - 128\left(\frac{\pi_5}{\pi_6}\right)\left[\pi_3^2\left(1 + \frac{1}{\pi_6}\right) - 1 - \frac{\pi_5}{\pi_6} - \frac{1}{\pi_6}\right](S\pi_2)^3$$

$$+ 16\left[\pi_3^2\left(1 + \frac{1}{\pi_6}\right)^2 - 1 - \frac{4\pi_5}{\pi_6} - \frac{2\pi_5}{\pi_6^2} - \frac{\pi_5^2}{\pi_6^2} - \frac{2}{\pi_6} - \frac{1}{\pi_6^2}\right](S\pi_2)^2$$

$$+ 8\left(1 + \frac{\pi_5}{\pi_6} + \frac{1}{\pi_6}\right)(S\pi_2) - 1 = 0 \tag{59}$$

As $\pi_6 \to 0$, the solution of equation (43) under the condition of equation (58) is

$$\left(\pi_{4,\,cr}\sqrt{\pi_2}\right)_{\pi_6=0} = \frac{1}{2}\sqrt{\frac{1+\frac{1}{\pi_5}}{1-\delta\pi_3}} \tag{60}$$

At the other extremity, when $\pi_6 = \infty$, equations (48) and (58) yield

$$\left(\pi_{4,\,cr}\sqrt{\pi_2}\right)_{\pi_6=\infty} = \frac{1}{2}\sqrt{\frac{1}{1-\delta\pi_3}} \tag{61}$$

Equation (60) reduces to equation (61) when π_5 becomes infinite.

RESULTS AND DISCUSSION

As previously mentioned, two classes of solution to the general frequency equations (eqs. (28) and (35)) exist. The determinant is a function of rotor rotational speed and shape; whereas its multiplying factor is independent of these parameters. This section presents graphical solutions and discussions of both the bouncing and conical modes of the frequency.

Bouncing Mode

The bouncing-mode frequency, obtained from equation (37), is the counterpart of the trivial solution $p/\sqrt{k_1/M} = 1$, which is one of the solutions of the frequency equation derived in the firm-foundation analysis of reference 1 when the center of gravity is midway between the bearings.

Figure 3 is a logarithmic plot of equation (37) that covers a range of the spring-constant ratio π_6 essentially from zero to infinity. The ordinate is the dimensionless frequency parameter $\pi_1 = p/\sqrt{k_1/M}$ defined by equation (29). The mass ratio $\pi_7 = M'/M$ varies over a range from one-half to infinity in figure 3. The upper set of solutions shown in figure 3 results from using the plus sign in equation (37). The minus sign yields the lower set.

The absence of rotor rotational speed and moment of inertia in figure 3 is worth discussing. Each set of two points on the curves of this figure at a given value of π_6 represents the bouncing-mode natural frequencies of one particular rotor configuration.

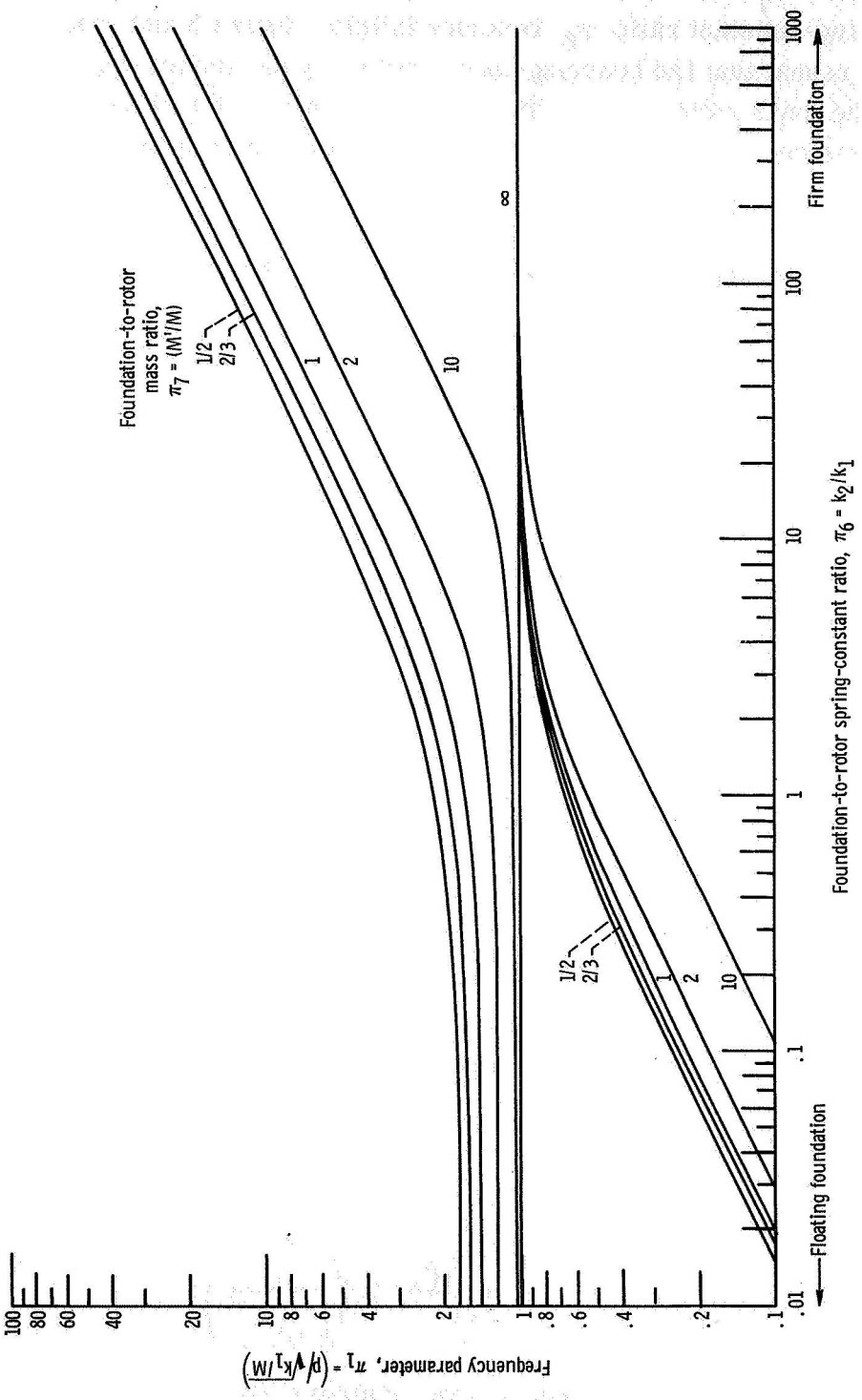

Figure 3. - Bouncing-mode natural-frequency plot (eq. (37)).

The magnitudes and existence of these frequencies are completely dissociated from the stationary or rotating condition of this particular rotor. Only the spring-constant ratio π_6 and mass ratio π_7 affect these solutions, as equation (37) and figure 3 both show.

As the spring-constant ratio π_6 becomes infinite, figure 3 and equation (37) with the minus sign reveal that the bouncing-mode frequency parameter approaches one. Likewise, as the mass ratio $\pi_7 \to \infty$, figure 3 and equation (37) with the plus sign show that π_1 becomes one. Physically, these two conditions correspond to the firm-foundation result $\pi_1 = 1$ found in reference 1.

At the other extremity in figure 3, where $\pi_6 \to 0$, the lower set of solutions vanishes. The upper set approaches the value $1 + (1/\pi_7)$, as equation (37) shows.

Conical Mode

The main discussion in this report is concerned with the conical-mode natural frequency, which is obtained mathematically when the determinant in equation (35) vanishes.

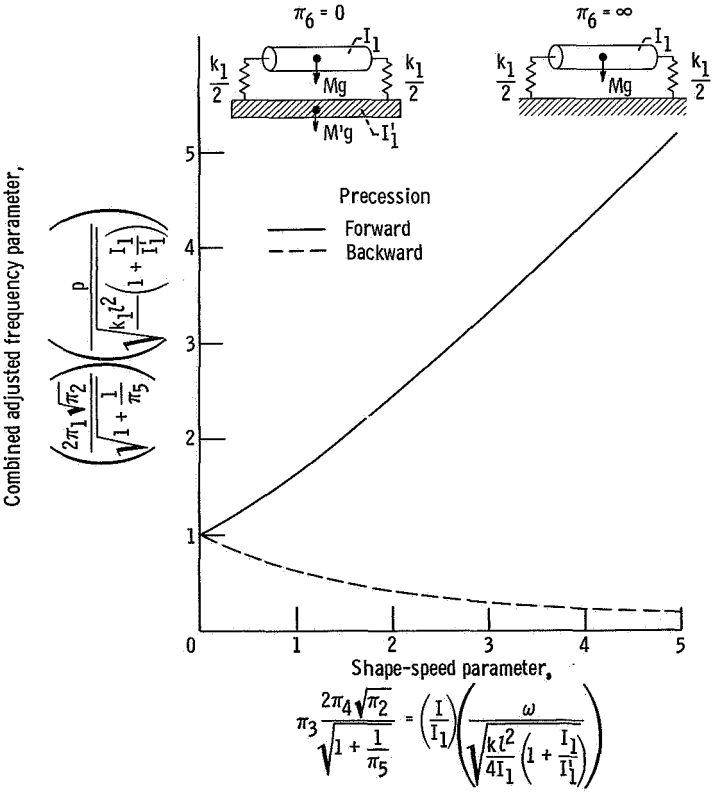

Figure 4. - Abbreviated solution (eq. (44) for $\pi_6 = 0$; eq. (49) for $\pi_6 = \infty$).

The solution is given by equation (40). It is evident that the foundation-to-rotor mass ratio π_7 is absent from this solution.

Prior to a discussion of the graphical solution of equation (40), consideration of special cases of the spring-constant ratio ($\pi_6 = 0$ and $\pi_6 = \infty$) is instructive. Application to aircraft and spacecraft for the condition $\pi_6 = 0$ was cited in connection with the derivation of equation (44) (see p. 13). The case $\pi_6 = \infty$ represents the firm-foundation model of reference 1.

Abbreviated solution. - Equation (44) is plotted in figure 4 with the factor $2/\sqrt{1 + (1/\pi_5)}$ multiplying $\pi_1\sqrt{\pi_2}$ in the ordinate and multiplying $\pi_3\left(\pi_4\sqrt{\pi_2}\right)$ in the abscissa. Inspection of equation (49) shows that figure 4 is also a graphical solution for this equation if the foundation-to-rotor moment-of-inertia ratio π_5 is assumed infinite in the coordinates. Therefore, a feature of figure 4 is that it applies to each of the two extreme cases (floating foundation, $\pi_6 = 0$ and firm foundation, $\pi_6 = \infty$). The set of curves in figure 4 is identical to a set in reference 1, with appropriate adjustment of coordinates.

The advantage of the form of solution given by figure 4 is that all geometries can be displayed by a single two-branch curve. The upper branch shown by the solid curve represents forward precession. The dotted curve represents backward precession. Figure 4 shows that as the adjusted shape-speed parameter increases, as by rising rotor rotational speed, the forward-precession frequency increases and the backward frequency decreases.

The point of intersection of the two branches in figure 4 locates graphically the zero-speed condition given analytically by equations (50) and (51). These results have therefore shown that a stationary rotor on a floating or firm foundation has two natural frequencies - one bouncing-mode frequency from equation (37) and one conical-mode frequency from equations (50) or (51).

From a comparison of equations (37) and (52), it is apparent that figure 3 also presents the geometric constraints for $\frac{1}{2}\sqrt{\left(1 + \frac{1}{\pi_5}\right)/\pi_2}$ that would be required for the zero-speed and bouncing-mode frequencies to be equal.

General solution. - Some example solutions of the general frequency equation (40) are presented graphically in figure 5. Representative samples appear in figure 5 with adjusted frequency parameter $\pi_1\sqrt{\pi_2}$ and adjusted shape-speed parameter $\pi_3\left(\pi_4\sqrt{\pi_2}\right)$ as coordinates. Presence of the disk effect π_2 in the coordinates reduces by two-thirds the number of plots needed to show the amount of information in figure 5 The foundation-to-rotor moment-of-inertia ratio $\pi_5 = I_1'/I_1$ is assigned values of 0.5, 1, and 3 in each part of figure 5. The spring-constant ratio $\pi_6 = k_2/k_1$ assumes constant values of 1/3, 1, and 2 in figures 5(a), (b), and (c), respectively.

For every value of π_5 on each plot in figure 5, there is a high-frequency set of so-

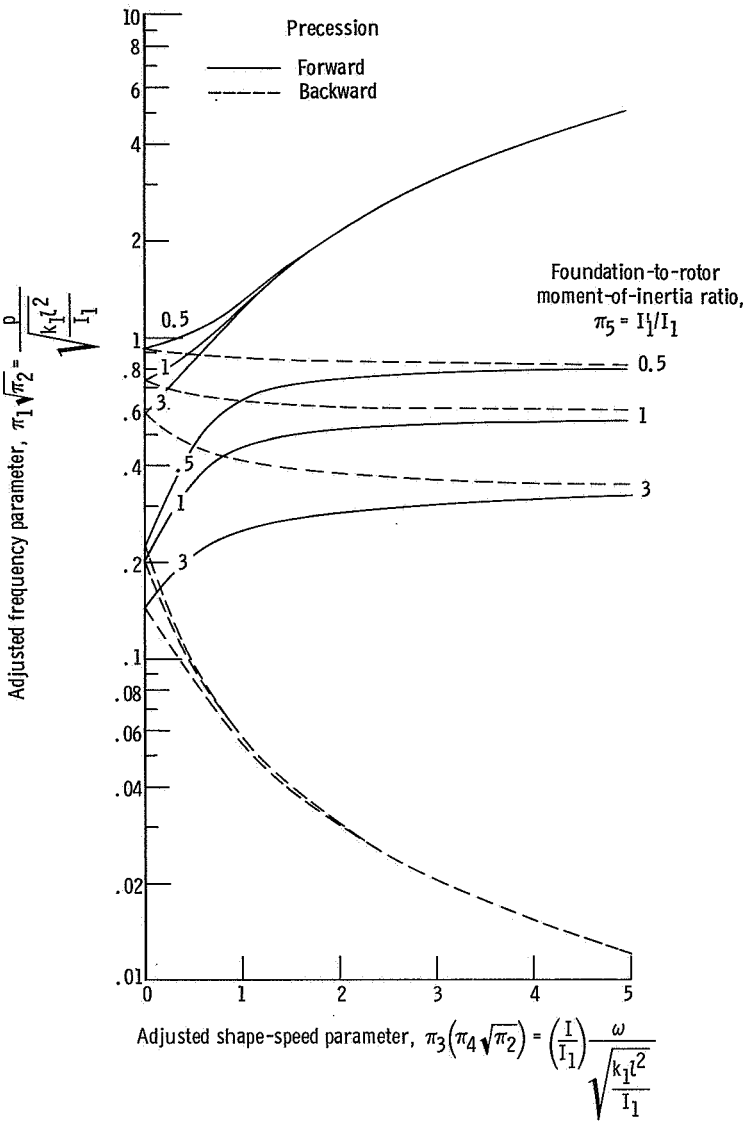

(a) Foundation-to-rotor spring-constant ratio, $\pi_6 = (k_2/k_1) = 0.3333$.

Figure 5. - General solution plots (eq. (40)).

lutions and a low-frequency set. For firm foundations, reference 1 reports only one set when the center of gravity is midway between the bearings. For given geometry, figure 5 shows four distinct solutions for $\pi_1\sqrt{\pi_2}$, except when $\pi_3\left(\pi_4\sqrt{\pi_2}\right) = 0$. The solid curves represent forward precession, while the dotted curves represent backward precession. The backward-precession curves rightly belong in the fourth quadrant but appear in the first quadrant for convenience. A mirror image of a general solution plot also exists in the second quadrant, but only repeats the information given in figure 5. These eight roots from figure 5 and its mirror image comprise the total implied by

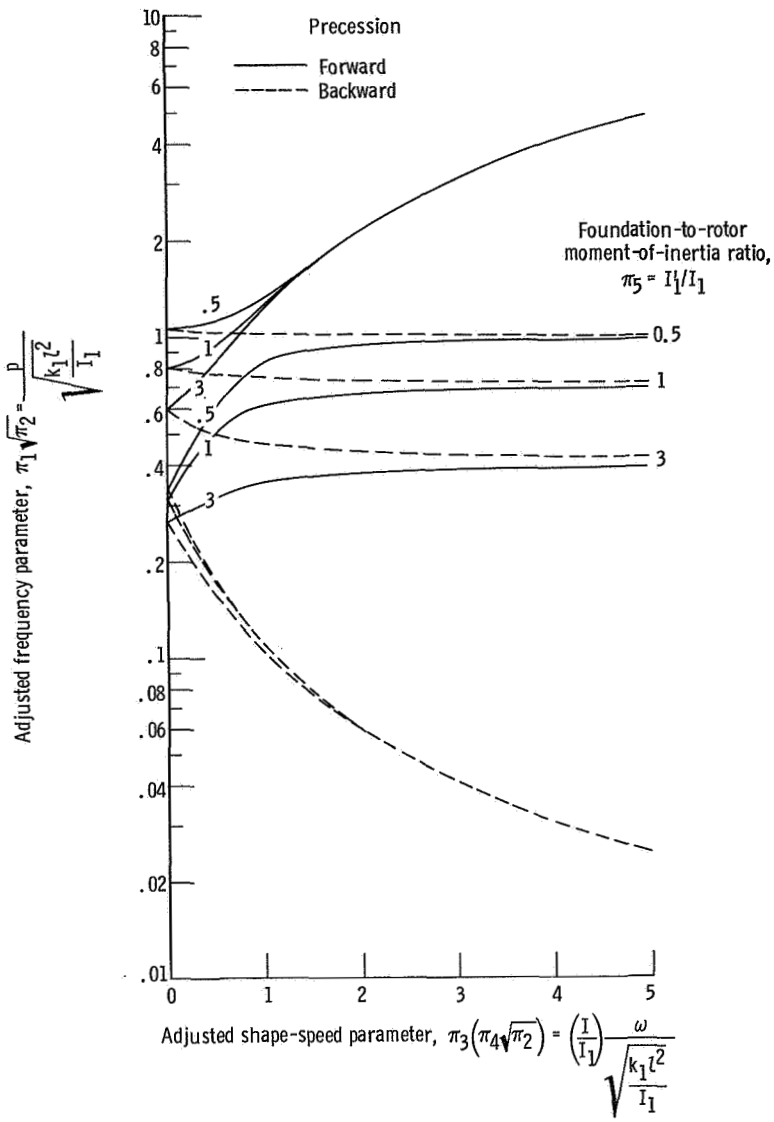

(b) Foundation-to-rotor spring-constant ratio, $\pi_6 = (k_2/k_1) = 1$.

Figure 5. - Continued.

equation (38). Because of the presence of π_2 and π_3 in the coordinates, each set of four points in figure 5 at a particular rotor rotational speed represents a single rotor configuration.

Comparison of figures 4 and 5 reveals a primary result of this investigation. This is an assessment of the extent of the error made by approximating a flexible-foundation configuration by a firm-foundation model. It is evident immediately that the flexible-foundation model predicts the existence of four frequency solutions, whereas the firm-foundation model predicts only two.

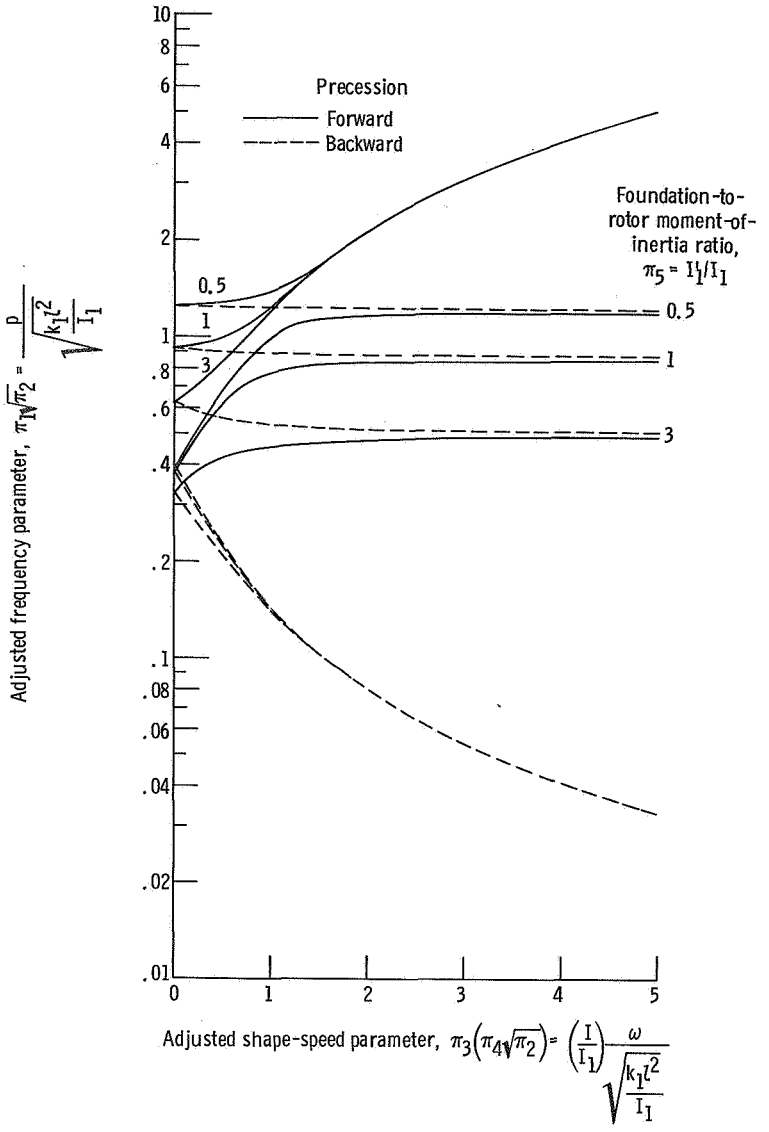

(c) Foundation-to-rotor spring-constant ratio, $\pi_6 = (k_2/k_1) = 2$.

Figure 5. - Concluded.

Table I compares quantitative results predicted by the two models. This table shows the approximate agreement between the flexible-foundation results and the two corresponding solutions of the firm-foundation model. Furthermore, such agreement exists over a wide range of spring-constant ratio π_6, as will be shown by the discussion on page 29.

Figure 5 illustrates the following trends when the effects of π_4, π_2, π_3, π_5, and π_6 are each isolated from all the others.

(1) When the rotational speed of a given rotor rises, the forward precession fre-

TABLE I. - COMPARISON OF FREQUENCY PARAMETERS PREDICTED BY FLEXIBLE- AND FIRM-FOUNDATION MODELS

Foundation model	Figure	π_5	π_6	$\pi_3\left(\pi_4\sqrt{\pi_2}\right)$	High-frequency set		Low-frequency set	
					[a]$\pi_1\sqrt{\pi_2}$	[b]$\pi_1\sqrt{\pi_2}$	[a]$\pi_1\sqrt{\pi_2}$	[b]$\pi_1\sqrt{\pi_2}$
Flexible	5(c)	1	2	2.5	2.6	0.88	0.84	-0.065
Firm	4	∞	∞	2.5	2.6	-----	----	-.10

[a]Forward precession.
[b]Backward precession.

quency increases and the backward frequency decreases.

(2) The frequency parameter π_1 is inversely proportional to the square root of the disk effect $\sqrt{\pi_2}$.

(3) The forward-precession frequency increases and the backward frequency decreases as the rotor polar-to-diametral moment-of-inertia ratio π_3 rises.

(4) The precession frequency decreases as the foundation-to-rotor moment-of-inertia ratio π_5 increases.

(5) When the foundation-to-rotor spring-constant ratio π_6 increases, the precession frequency increases.

When the adjusted shape-speed parameter $\pi_3\left(\pi_4\sqrt{\pi_2}\right)$ becomes large, all the forward-precession high-frequency curves in figure 5 approach as an asymptote the relation expressed by equation (42). Figure 5 also shows the asymptote approached by backward precession in the low-frequency set, as expressed in equation (41).

In figure 5, there is a zero-speed condition for each of the two sets, given by the intersections of the branches. Therefore, a stationary rotor on a flexible foundation has four natural frequencies, including the two bouncing-mode solutions.

Frequency plots. - A graph of the variation in adjusted frequency parameter $\pi_1\sqrt{\pi_2}$ with adjusted rotational-speed parameter $\pi_4\sqrt{\pi_2}$ is called a frequency plot. It is easily constructed from a general solution plot by specifying values for the rotor moment-of-inertia ratio, π_3 for use as a parameter as in figure 6. In this figure, which was derived from figure 5(c), π_5 is 3 and π_6 is 2. Therefore, figure 6 is less general and presents less information than figure 5(c).

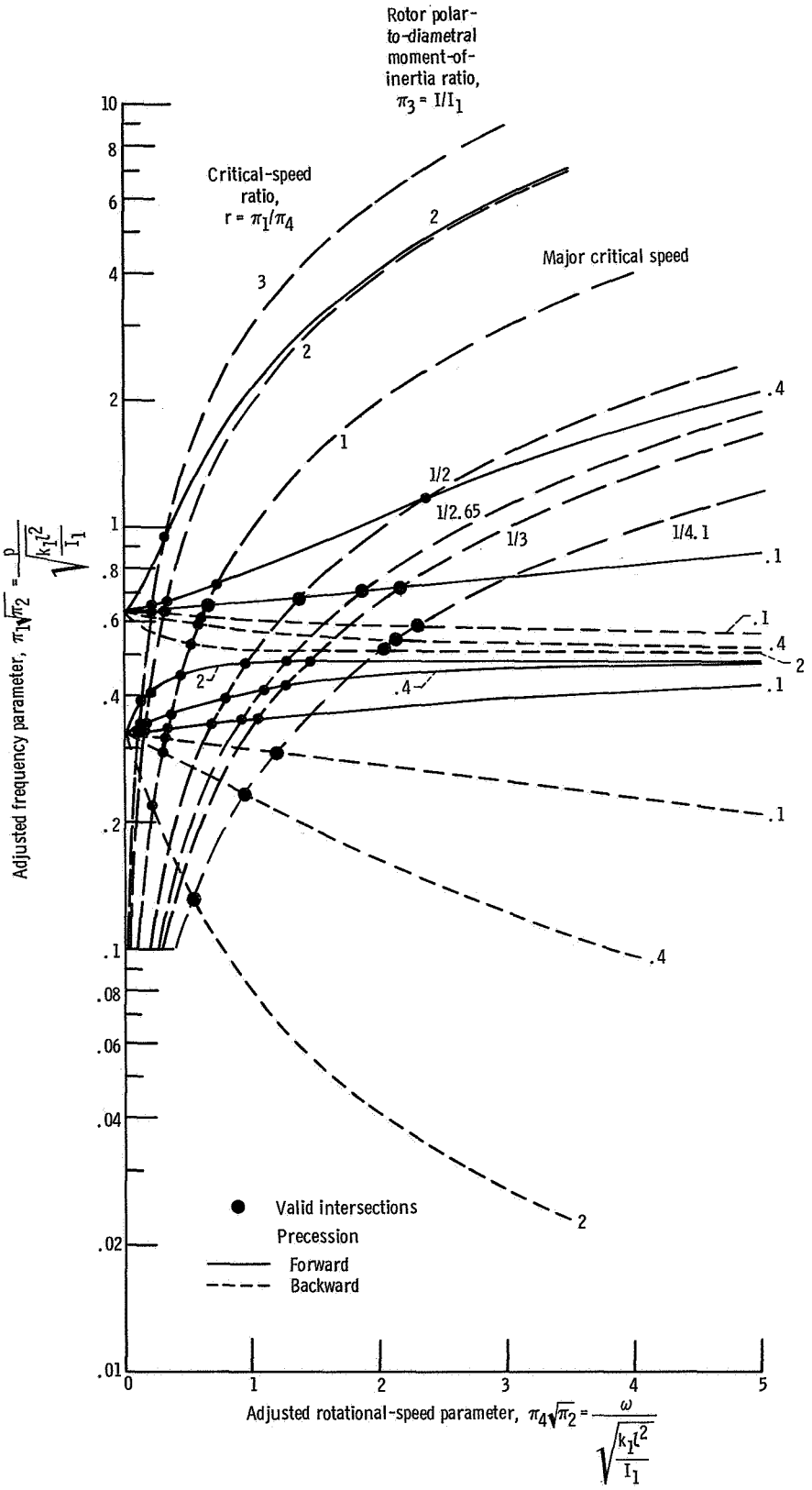

Figure 6. - Frequency plot. $\pi_5 = I_1'/I_1 = 3$; $\pi_6 = k_2/k_1 = 2$.

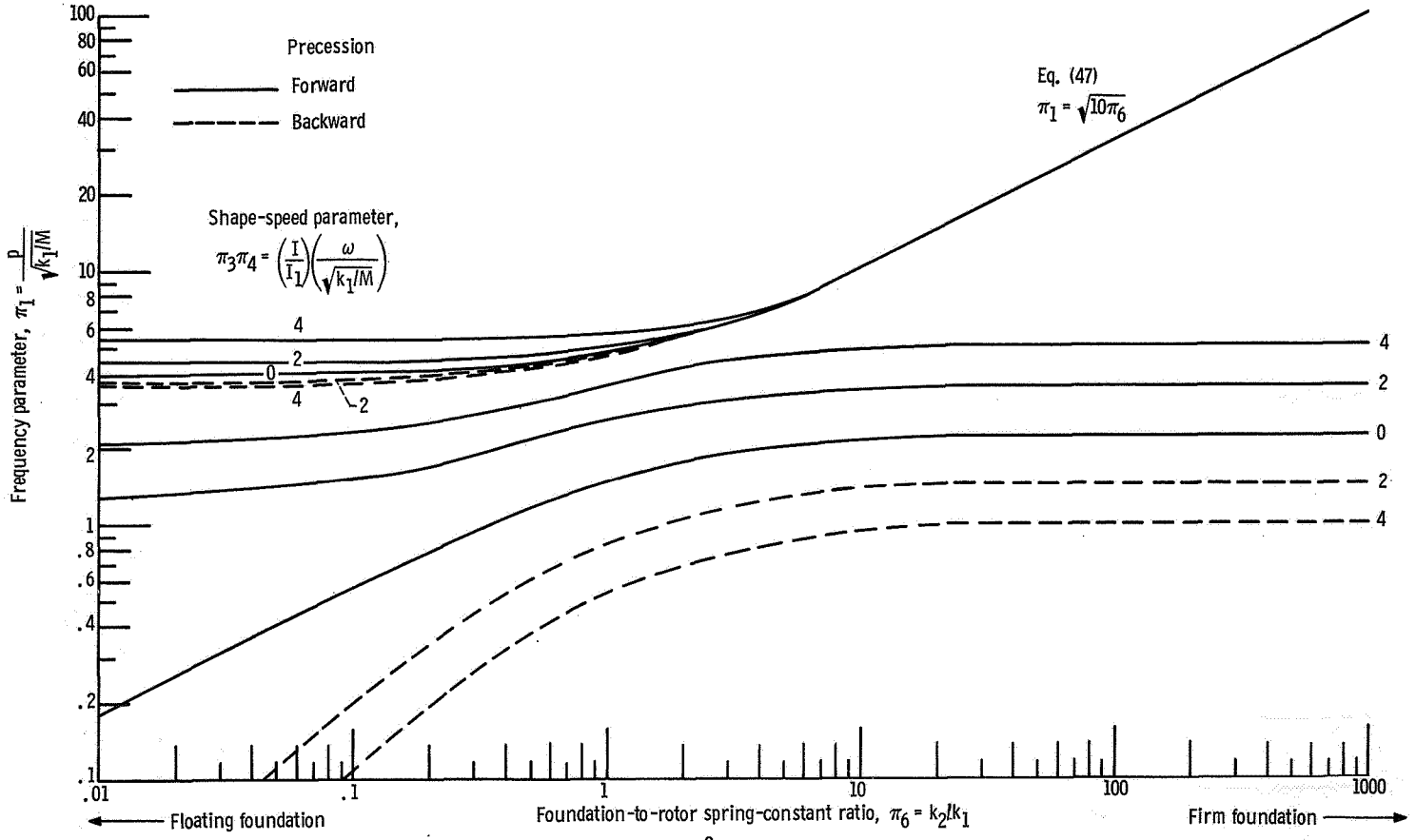

(a) $\pi_2 = I_1/ML^2 = 0.05$; $\pi_5 = I_1'/I_1 = 0.5$.

Figure 7. - Spring-constant plots.

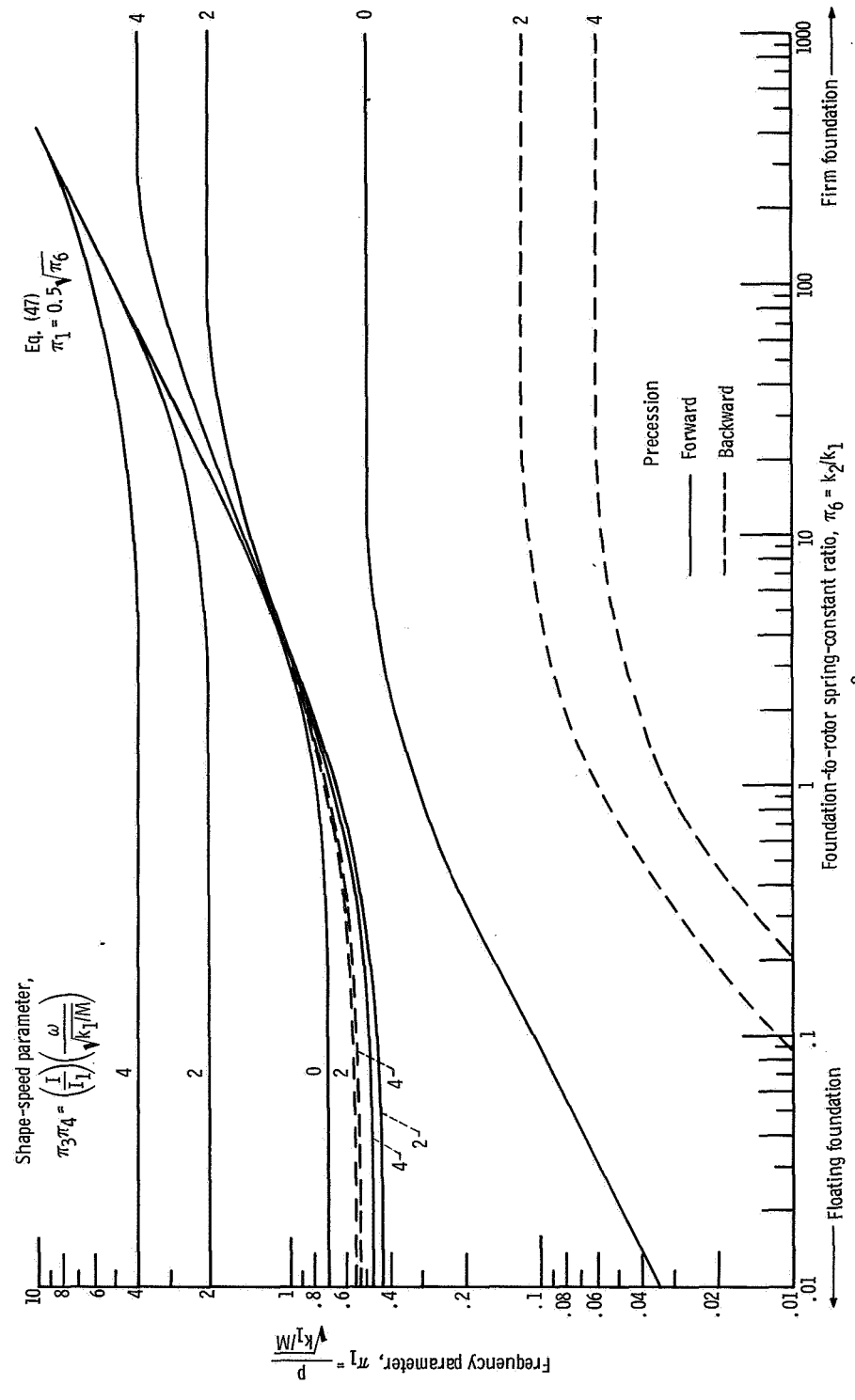

(b) $\pi_2 = I_1/ML^2 = 1$; $\pi_5 = I_1'/I_1 = 1$.

Figure 7. - Concluded.

Frequency plots are convenient for locating critical speeds by intersections of critical-speed ratio curves and frequency curves. Several critical-speed ratio curves appear in figure 6. Their significance will be treated in the nonsynchronous critical-speed discussions (see pp. 39 and 40). Each constant π_3 curve on a frequency plot represents the behavior of a particular rotor, and shows its passage through various critical speeds during rotor rotational-speed changes.

The gradual slope of the low-value π_3 curves in figure 6 shows that variation in rotor rotational speed has little effect on the precession of pencil-shape rotors. This observation is also true for high- and low-frequency backward precession of all shapes.

Spring-constant plots. - An overall perspective of the effect of variations in the foundation-to-rotor spring-constant ratio π_6 on the frequency parameter π_1 is provided by spring-constant plots, two of which appear in the logarithmic graphs of figure 7. This figure uses the shape-speed parameter $\pi_3\pi_4$ as the parametric variable. Figure 7(a) applies to any geometry in which $\pi_2 = 0.05$ and $\pi_5 = 0.5$, while 7(b) applies to any geometry in which $\pi_2 = 1$ and $\pi_5 = 1$. Figure 7 covers a range in spring-constant ratio π_6 from essentially zero to infinity. Figure 4 provides the totality of solutions for both the lower and upper boundaries of π_6 in figure 7.

The flatness of the curves in figure 7 account for the agreement between the firm- and flexible-foundation models shown in table I. Figure 7 shows close agreement of the high-frequency forward-precession curves over a wide range of spring-constant ratio π_6 with the low-frequency forward-precession curves at their firm-foundation limits. Likewise, the low-frequency backward-precession curves in figure 7 are insensitive to variation in π_6 above values for π_6 of about 1.

As the spring-constant ratio π_6 increases, the curves of constant $\pi_3\pi_4$ of the high-frequency set approach asymptotically the relation given by equation (47), as shown in figure 7. On a logarithmic plot of π_1 against π_6, equation (47) maps as a straight line.

As π_6 increases, the curves of the low-frequency set in figure 7 approach values given by figure 4 and equation (49) with zero slope.

Thus, for floating foundations, the solutions provided by figure 4 correspond to the high-frequency set. For firm foundations, the figure 4 solutions correspond to the low-frequency set.

Figure 8 is an expanded portion of figure 7(a), showing the region about $\pi_6 = 0$ in rectangular coordinates.

To summarize, plots such as those in figure 7 provide solutions for the entire range

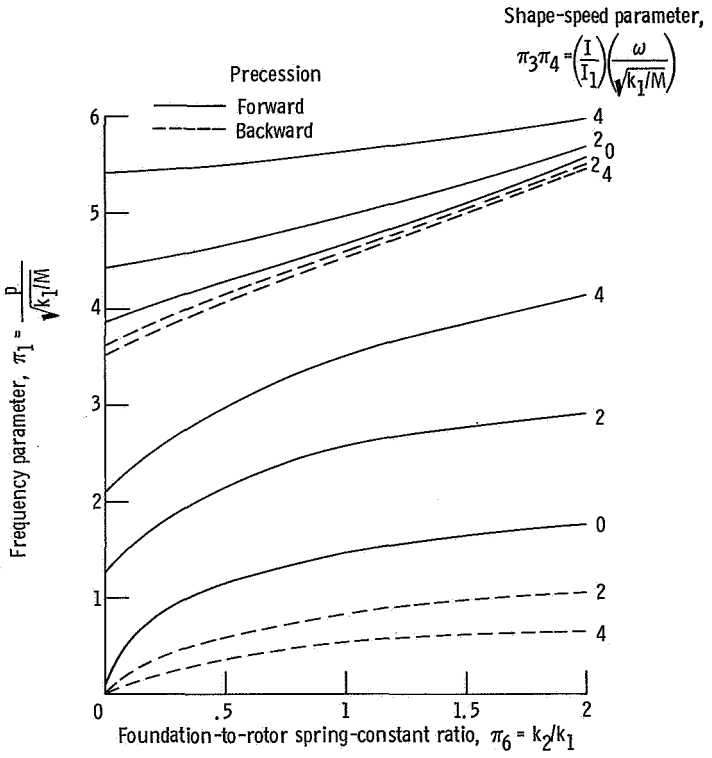

Figure 8. - Enlarged section of spring-constant plot of figure 7(a). $\pi_2 = I_1/Ml^2 = 0.05$; $\pi_5 = I_1'/I_1 = 0.5$.

of geometry, speed, and spring-constant ratio. Use of only three values of spring-constant ratio π_6 in calculation of the general frequency equation (40) suffice in production of any one of these plots for the following reasons. The Den Hartog-type plot of figure 4 establishes the lower and upper extremities of π_6 in figure 7. The high-frequency curves approach asymptotically the expression given by equation (47) as π_6 increases.

Asymptotic limit. - Figure 9 is a graphical representation of the asymptotic limit given by equation (47). This figure shows that the parabolic relation between π_1 and π_6 is linear with a slope of 0.5 for all values of $\pi_2\pi_5$ on a logarithmic plot, as taking the log of equation (47) verifies. As is evident from figure 7, the asymptotic limit forms the backbone of the spring-constant plots.

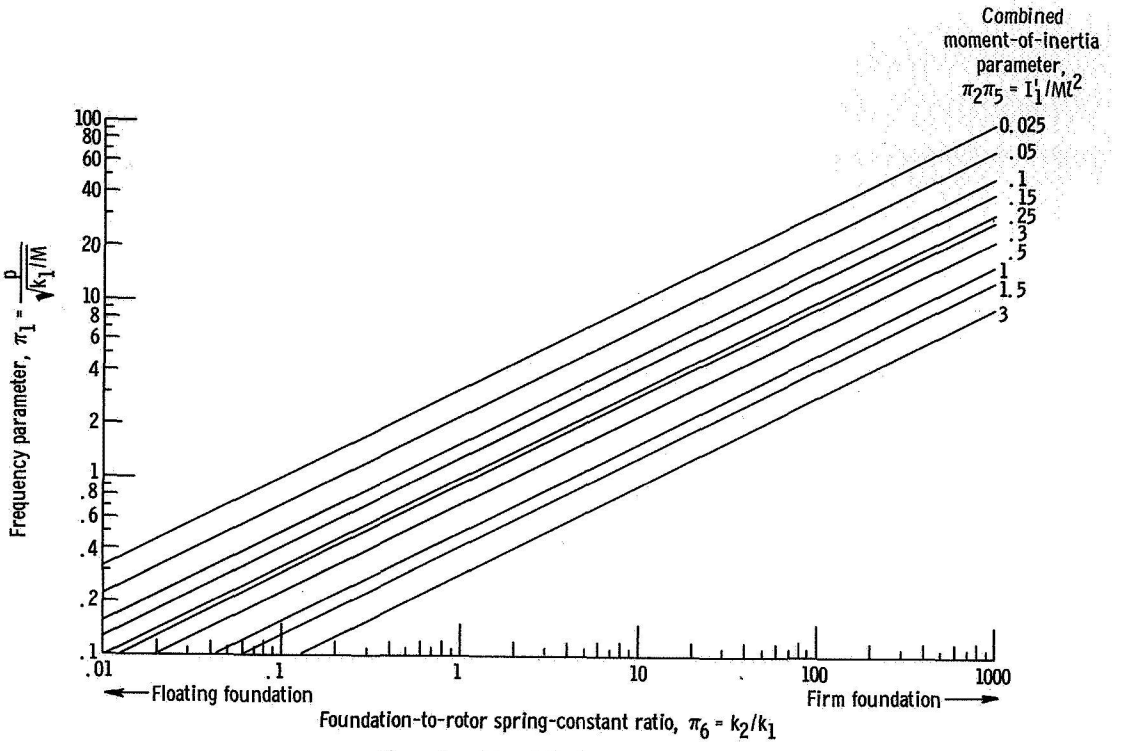

Figure 9. - Asymptotic limits (eq. (47)).

Major Critical Speeds

A practical application of the theory and maps developed in this report is to use them to locate major critical speeds. Knowledge of major critical-speed conditions is important because large vibration-amplitudes occur at major critical speeds in the absence of damping. Major critical speed is defined by equation (58)

Major critical-speed conditions are most easily visualized by referring to a frequency plot, such as figure 6. On a frequency plot, intersections of the critical-speed ratio curve $r = 1$ with the frequency curves establish the major critical speeds. The trace of a major critical-speed curve on a general solution plot, such as figure 5, is given by

$$\frac{\pi_1 \sqrt{\pi_2}}{\pi_3\left(\pi_4 \sqrt{\pi_2}\right)} = \frac{1}{\pi_3} \tag{62}$$

Effect of shape. - A less pictorial but more mathematically rigorous approach to locating the major critical speeds is provided by equation (59). Graphical solutions of this equation appear in figure 10, which uses $\pi_{4,\,cr}\sqrt{\pi_2}$ and π_3 as coordinates. The

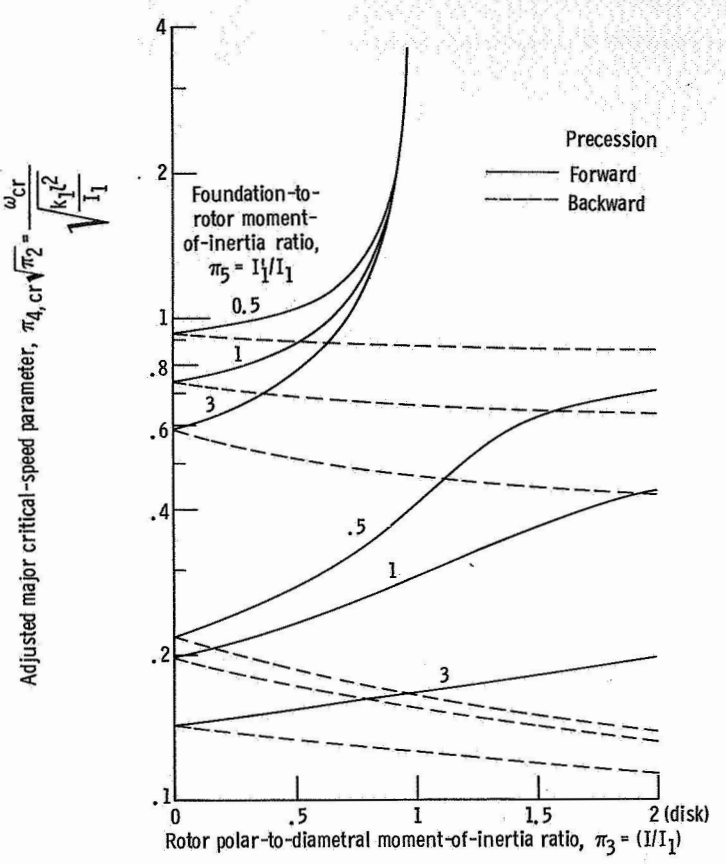

(a) Foundation-to-rotor spring-constant ratio, $\pi_6 = (k_2/k_1) = 0.3333$.

Figure 10. - Adjusted major critical-speed plots (eq. (59)).

parameter π_5 varies in figure 10 to show the effect of rotor shape on major critical speed. The spring-constant ratio is fixed in figure 10(a) at 0.333, in 10(b) at 1.0, and in 10(c) at 2.0.

Trends (2) to (5) enumerated in the General solution section (pp. 24 and 25) also apply to major critical speeds, as figure 10 shows.

All the forward-precession curves of the high-frequency sets in figure 10 approach infinity as $\pi_3 \to 1$. This circumstance is related to the discussion of the roots of equation (54) (see p. 17). Therefore, because no real solutions exist for $\pi_3 \geq 1$, forward

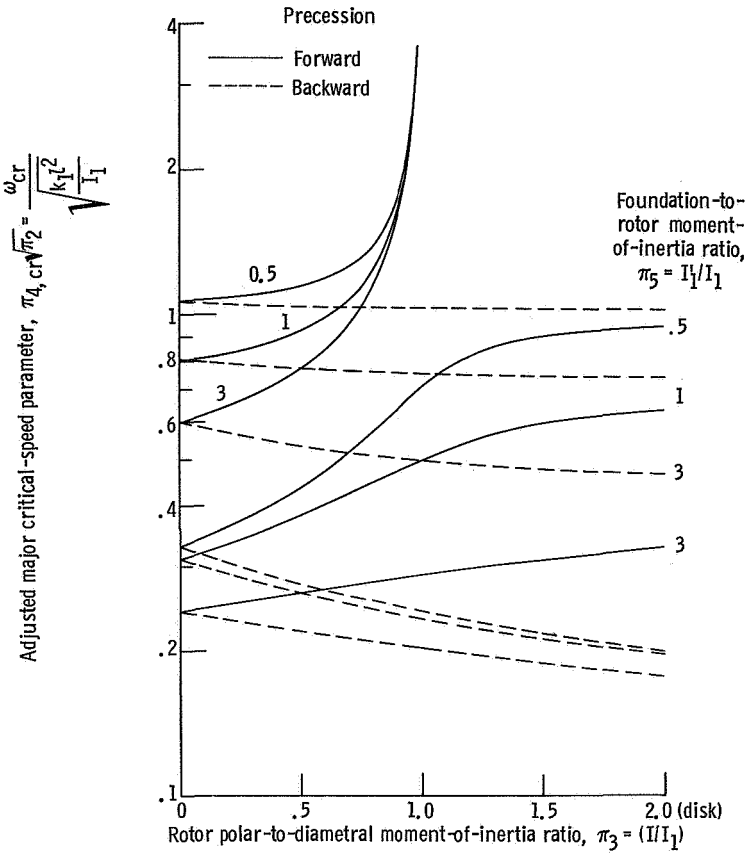

(b) Foundation-to-rotor spring-constant ratio, $\pi_6 = (k_2/k_1) = 1$.

Figure 10. - Continued.

major critical speed of the high-frequency set can be avoided by using such designs. If this is not feasible, designing with π_3 as close to one as possible may yield a major critical speed well above the design rotor rotational speed.

Selective geometrical design can not so easily avoid backward major critical-speed resonances, as shown by the fact that the dashed curves in figure 10 remain finite over the entire range of π_3. The presence of $\sqrt{\pi_2}$ in the ordinate of figure 10, however, suggests that if a design with a low value of π_2 is used (pencil shapes), both the forward and backward major critical speeds may be high enough to exceed design speed.

Effect of spring-constant ratio. - Figure 11 presents the effect of spring-constant ratio π_6 on $\pi_{4,cr}\sqrt{\pi_2}$ with curves of constant values of π_5. A pencil-shape rotor $\pi_3 = 0.1$ appears in figure 11(a), and a disk $\pi_3 = 2$ is represented in figure 11(b).

Figure 11 gives an overall perspective of major critical-speed conditions. The

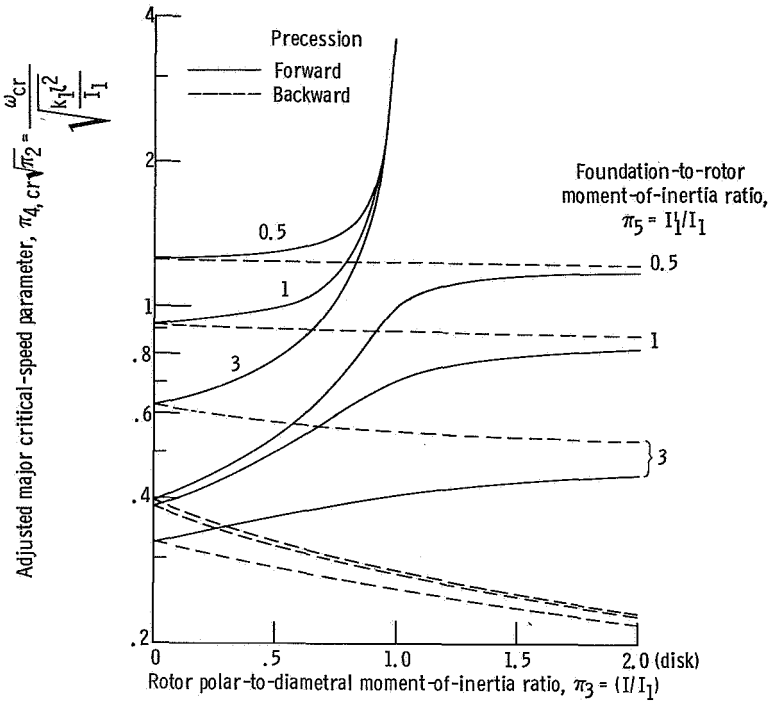

(c) Foundation-to-rotor spring-constant ratio, $\pi_6 = (k_2/k_1) = 2$.

Figure 10. - Concluded.

curves at the lower extremities of π_6 are approximated by equation (60), and at the upper by equation (61). The asymptotes approached by the high-frequency set are plotted from equation (47).

No high-frequency forward-precession curves appear in figure 11(b) because $r < \pi_3$ (see p. 17). As π_6 becomes large, the low-frequency curves in figure 11(a) converge into one forward- and one backward-precession curve (eq. (61)). The backward-precession curves of figure 11(b) behave like those in figure 11(a). The low-frequency forward-precession curves of figure 11(b) merge into their respective asymptotes as π_6 becomes large, as equation (47) specifies.

There are no regions in the quadrant represented by figure 11 in which critical-speed solutions are forbidden. In figure 11(a), as $\pi_5 \to 0$ the low-frequency curves approach the constant value of equation (61) for all values of π_6. This observation also is true for the low-frequency backward-precession curves of figure 11(b). But when $\pi_3 > r$ (fig. 11(b)), the low-frequency forward-precession curves approach the ordinate axis (not shown) as $\pi_5 \to 0$.

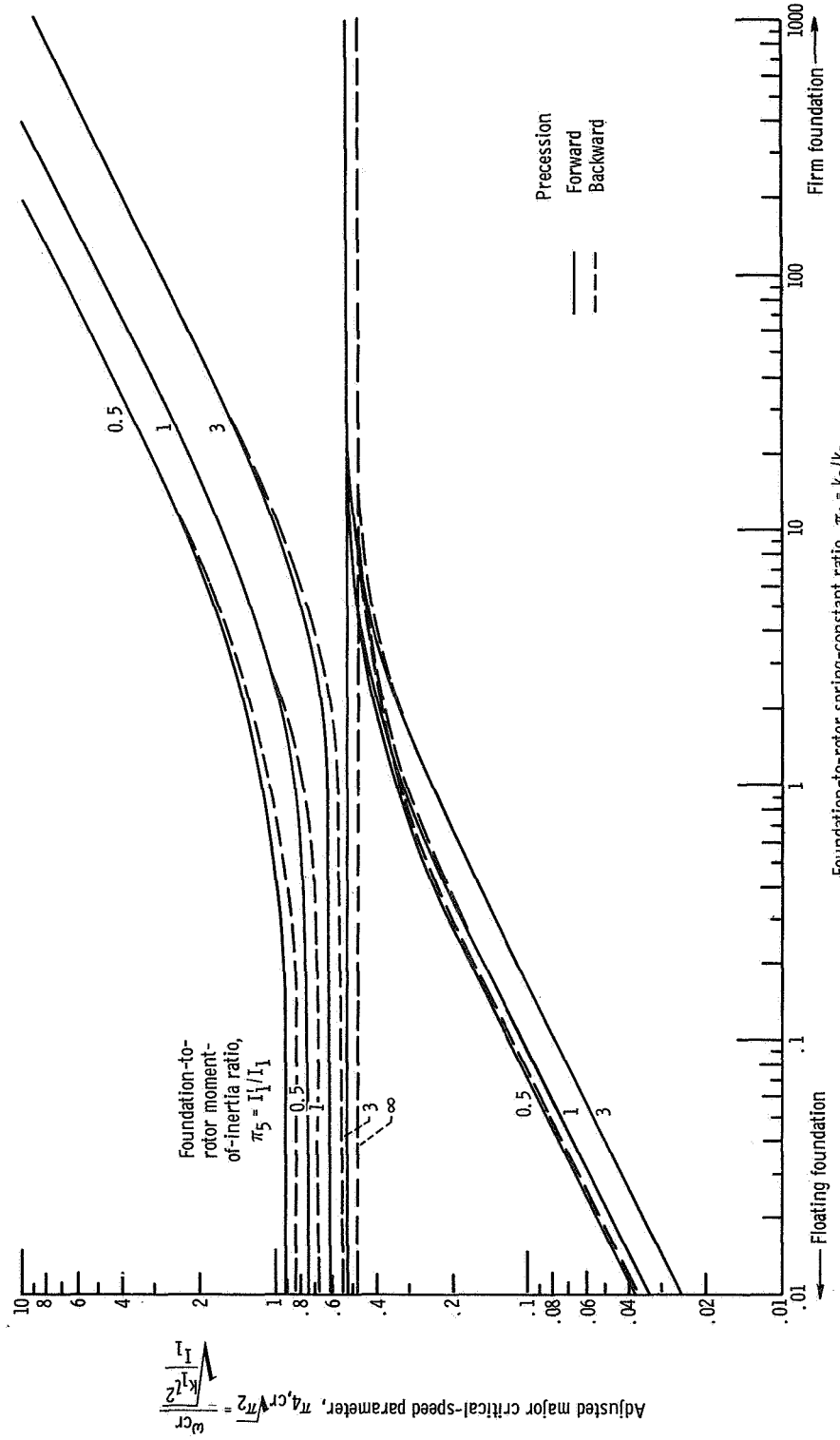

(a) Pencil shape; $\pi_3 = I/I_1 = 0.1$.

Figure 11. - Effect of spring-constant ratio on major critical speed.

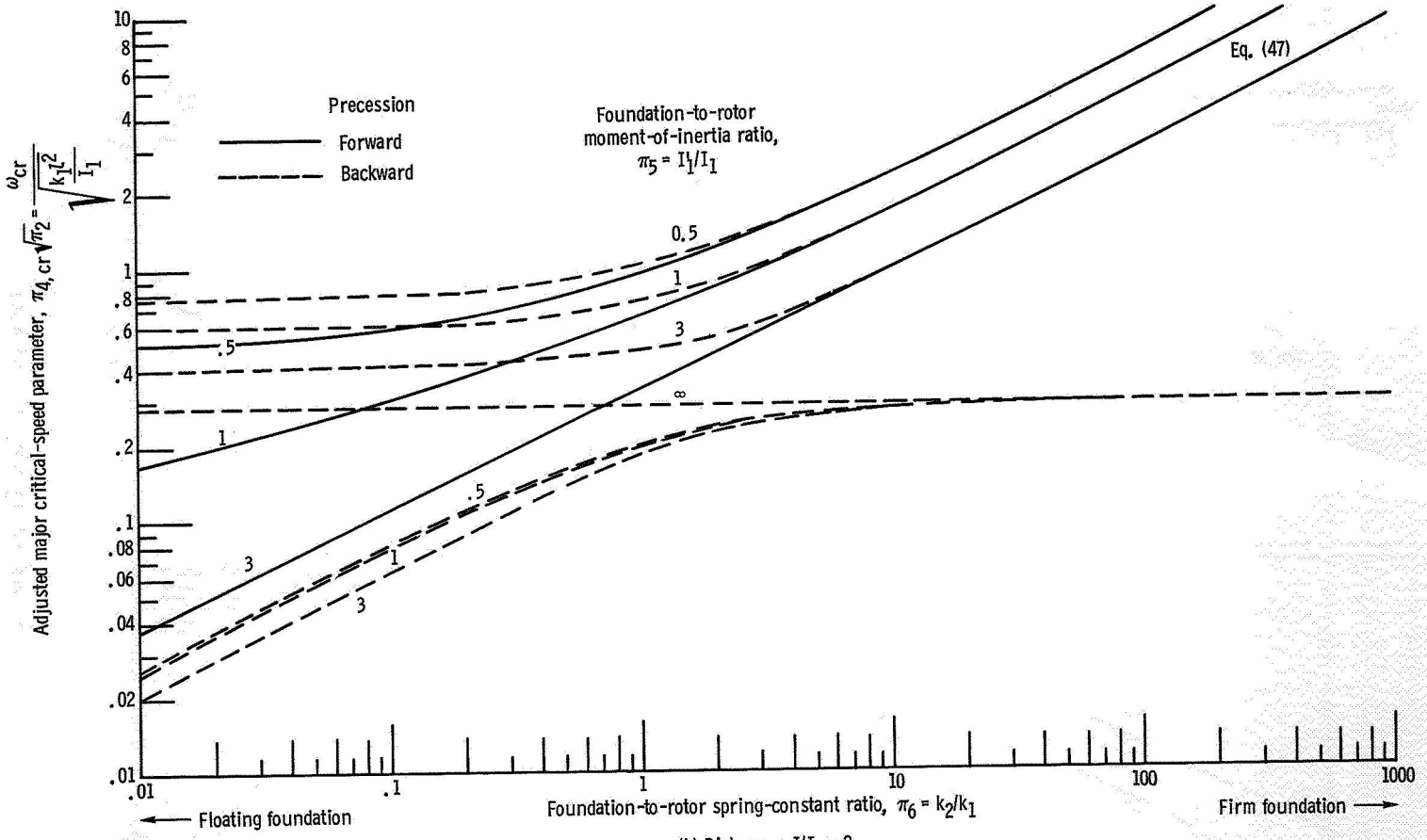

(b) Disk; $\pi_3 = I/I_1 = 2$.

Figure 11. - Concluded.

As π_5 increases, the low-frequency set covers the lower region of figure 11 all the way down to the abscissa axis (not shown). As $\pi_5 \to 0$, curves of the high-frequency set approach infinity in figure 11. At the other extreme, they approach the constant value given by equation (61) as π_5 becomes infinite.

Because of the trends observed in figure 7, it was expected that for a given geometry the major critical speeds shown in figure 11 would increase with an increase in π_6.

Rising rotor rotational speed is represented in figure 11 by a traverse upward on the map at constant π_6. Such a movement from a π_5 curve of the low-frequency set to the corresponding π_5 curve of the high-frequency set locates successive major critical speeds.

Abbreviated major critical-speed plot. - Just as the abbreviated frequency plot in figure 4 set the extreme boundaries of figure 7, the abbreviated major critical-speed plot in figure 12 does likewise for figure 11. With the ordinate $2\pi_{4,\,cr}\sqrt{\pi_2}/\sqrt{1 + (1/\pi_5)}$, figure 12 is a plot of equation (60) for which $\pi_6 = 0$ (floating foundation). When π_5 is set at infinity, figure 12 represents equation (61), for which $\pi_6 = \infty$ (firm foundation). The rotor moment-of-inertia ratio π_3 is the abscissa coordinate in figure 12. It varies

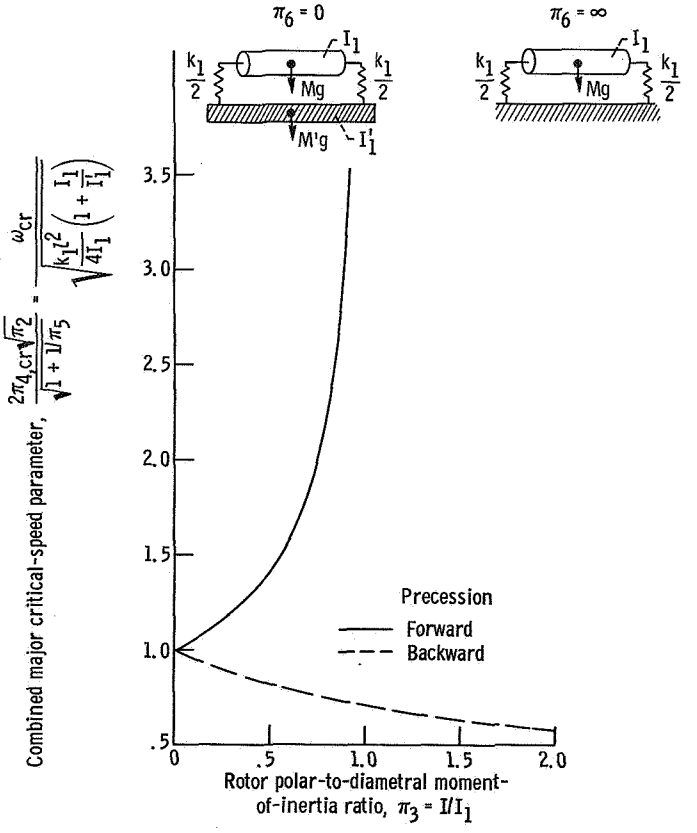

Figure 12. - Abbreviated major critical-speed plot (eq. (60) for $\pi_6 = 0$; eq. (61) for $\pi_6 = \infty$).

TABLE II. - COMPARISON OF MAJOR CRITICAL SPEEDS PREDICTED BY FLEXIBLE- AND FIRM-FOUNDATION MODELS

Foundation model	Shape	Figure	π_5	π_6	π_3	High-frequency set		Low-frequency set	
						[a] $\pi_{4,\,cr}\sqrt{\pi_2}$	[b] $\pi_{4,\,cr}\sqrt{\pi_2}$	[a] $\pi_{4,\,cr}\sqrt{\pi_2}$	[b] $\pi_{4,\,cr}\sqrt{\pi_2}$
Flexible	Pencil	10(c)	1	2	0.1	0.93	-0.91	0.40	-0.37
Firm	Pencil	12	∞	∞	.1	(1)	(-1)	.52	-.47
Flexible	Disk	10(c)	1	2	2	----	-.88	.83	-.23
Firm	Disk	12	∞	∞	2	----	(-1)	----	-.29

[a] Forward precession.
[b] Backward precession.

from zero to the value for a disk (2). Again, as in figure 10, the high-frequency curve approaches infinity as $\pi_3 \to 1$, beyond which this curve does not exist.

Comparison with firm-foundation results. - Table II presents a comparison of the major critical speeds predicted by the two models for both pencil-shape rotors and disks. In table II, the two solutions not predicted by the firm-foundation model are approximated by using plus and minus the firm-foundation bouncing-mode solution. The reasonably good agreement between the two sets of results for both pencil-shape rotors and disks implies good agreement for all intermediate shapes. Table II has thus shown that the firm-foundation results from figure 12 with the addition of this model's bouncing-mode solutions (±1) provide an easily obtained but good approximation to flexible-foundation results.

Nonsynchronous Critical Speeds

In references 6 to 9, Yamamoto reports on experimental work showing that large amplitude increases occur at rotor rotational speeds other than the major critical. His work with rotors supported by ball bearings revealed that bearing defects cause nonsynchronous precession. He found two classes of nonsynchronous precession associated with double-row ball bearings (refs. 6 and 7), and two other classes associated with single-row types (refs. 8 and 9).

With double-row ball bearings, nonsynchronous critical speeds occur both above and below the major critical speed. All nonsynchronous critical speeds associated with single-row ball bearings occur at rotor rotational speeds greater than the major critical. The spring characteristics of double-row ball bearings are linear, and those of the

single-row type are nonlinear.

Double-row ball bearings. - Nonuniformity in ball diameters is a cause of nonsynchronous motion at rotor rotational speeds greater than the major critical. Yamamoto's work disclosed that the most serious conditions of this type occur when

$$r = \frac{1}{2.65} \tag{63}$$

for forward precession, and

$$r = -\frac{1}{4.1} \tag{64}$$

for backward precession.

Frequency plots, such as the example shown in figure 6, are ideally suited for displaying critical-speed conditions. Curves of constant critical-speed ratio r could also be shown on the general solution plots of figure 5.

Curves representing equations (63) and (64) appear in figure 6. Only the intersections of equation (63) with the forward-precession curves are meaningful. Similarly, the intersections of equation (64) with backward-precession curves are meaningful. Dots in figure 6 denote valid intersections. For a given rotor, the nonsynchronous critical speeds specified by equations (63) and (64) are more than twice the major critical speeds.

Yamamoto showed that noncircular inner and outer bearing races cause nonsynchronous motion at critical-speed ratios r of 2, 3, and 5. Because of the small amplification that occurs at $r = 5$, this condition is not serious. Curves depicting $r = 2$ and $r = 3$ appear in figure 6. According to Yamamoto, only the intersections with forward-precession curves are valid. Because all intersections occur well below the major critical speed, even low-speed rotors can experience this type of nonsynchronous precession during acceleration.

Inspection of the curve for $\pi_3 = 2$ in figure 6 reveals that no high-frequency forward-precession intersections occur for critical-speed ratios $r \leq 2$. This is a graphical illustration of the fact discussed in connection with equation (54) that one of the solutions for $\pi_1\sqrt{\pi_2}$ is imaginary when $\pi_3/r \geq 1$. Thus, as reference 1 reported, no high-frequency forward-precession critical speed can exist for geometries in which π_3 equals or exceeds the critical-speed ratio. Low-frequency critical speeds exist, however, for all rotor shapes.

It is not likely that a set of double-row ball bearings will have only one of the two types of defects mentioned. It may therefore be presumed that nonsynchronous critical speeds defined by equations (63) and (64), and $r = 2$ and 3 will all occur.

Single-row ball bearings. - Yamamoto observed in reference 8 that nonsynchronous critical speeds of subharmonic oscillation appear only when the shafts are supported by single-row ball bearings. This motion, which appears only in forward precession, results from nonsymmetry of the nonlinear spring characteristics of the bearings.

Subharmonic motion is characterized by critical-speed ratios $r = 1/2,\ 1/3,\ 1/4,\ \ldots\ 1/n$, where n is a positive real integer. This phenomenon can occur only after the major critical speed is exceeded because $r < 1$ (see fig. 6). Also, because of the low value of r, pencil-shape rotors experience both high- and low-frequency motion of this type. Only low-frequency precession is possible in disks. Figure 6 shows curves of $r = 1/2$ and $r = 1/3$ to provide examples of this phenomenon.

Yamamoto further observed in references 8 and 9 that when single-row ball bearings are used, two natural frequencies build up together at certain rotor rotational speeds. The absolute value of their sum or difference is related to rotor rotational speed by

$$\omega = |p_i \pm p_j| \tag{65}$$

in which p_i and p_j are any two of the four natural frequencies obtained from equation (54). Yamamoto refers to this motion as summed and differential harmonic oscillations. In reference 8, Yamamoto reports that vibration amplitudes from these sources may exceed those of the major critical speeds. From figure 5, it is evident that the condition $i = j$ is trivial and applies only at zero rotational speed.

Because there are four unique solutions p_1, p_2, p_3, and p_4 to the frequency equation, there are 12 summed and differential combinations of the type specified in equation (65). To display these combinations graphically, figure 13 presents the portion of the frequency plot of figure 6 pertaining to $\pi_3 = 0.4$. Solutions p_1 and p_2 represent forward precession and p_3 and p_4 represent backward precession. The curve $r = 1$ locates nonsynchronous critical speeds of this type in figure 13. Because the intersections of all curves with the curve $r = 1$ in figure 13 are valid, it is unnecessary to use dots.

At zero rotor rotational speed, solutions p_1 and p_4 coincide as do p_2 and p_3. Therefore, there can be no intersections of the curve $r = 1$ with the curves $|p_1 + p_4|$ and $|p_2 + p_3|$, as figure 13 shows. These solutions are forbidden for any geometry from pencil shape to disk. Figure 13 shows that the maximum number of intersections is 10 for any shape.

Yamamoto and Hayashi proved mathematically in reference 9 that only summed harmonic oscillations can occur if both frequencies p_i and p_j represent forward precession, or if both represent backward precession. Only differential harmonic oscillations can occur if one frequency represents forward and the other represents backward precession. Table III reviews the combinations allowed and forbidden.

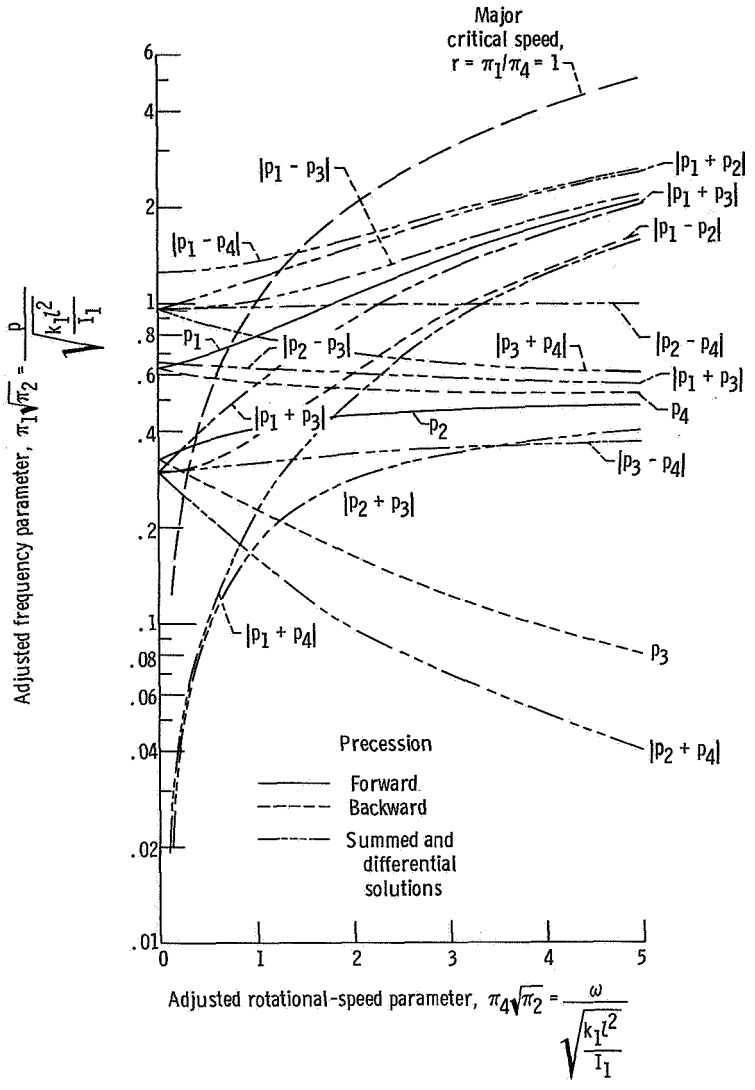

Figure 13. - Frequency plot locating summed-and-differential harmonic nonsynchronous critical speeds. $\pi_3 = I/I_1 = 0.4$; $\pi_5 = I_1'/I_1 = 3$; $\pi_6 = k_2/k_1 = 2$.

TABLE III. - ALLOWED AND FORBIDDEN SUMMED AND DIFFERENTIAL HARMONIC COMBINATIONS

Allowed					
$\lvert p_1 + p_2 \rvert$	$\lvert p_1 - p_3 \rvert$	$\lvert p_1 - p_4 \rvert$	$\lvert p_2 - p_3 \rvert$	$\lvert p_2 - p_4 \rvert$	$\lvert p_3 + p_4 \rvert$
Forbidden					
$\lvert p_1 - p_2 \rvert$	$\lvert p_1 + p_3 \rvert$	$\lvert p_1 + p_4 \rvert$	$\lvert p_2 + p_3 \rvert$	$\lvert p_2 + p_4 \rvert$	$\lvert p_3 - p_4 \rvert$

For disks, no $|p_1 \pm p_j|$ intersections can exist, as figure 6 verifies. These intersections are nonexistent for any rotor shapes for which $\pi_3 \geq 1$. Consequently, for disks only 5 intersections of $|p_i \pm p_j|$ with the curve $r = 1$ are possible. But table III forbids two of these. Therefore, only $|p_2 - p_3|$, $|p_2 - p_4|$, and $|p_3 + p_4|$ can occur for disks. Yamamoto and Hayashi present experimental evidence in reference 9 to substantiate table III for disks.

A conclusion from this phase of the study is that the maximum number of summed and differential nonsynchronous critical speeds is 3 for disks and 6 for pencil-shape rotors. These results coincide with those found in reference 1 for a firm-foundation model.

From figure 6 it can be shown that for $\pi_3 = 1$, the curve $\omega = |p_1 + p_3|$ lies close to the curve $r = 1$ over most of the speed range. Fortunately, table III forbids a nonsynchronous critical speed for these conditions. Therefore, this potential danger does not occur.

SUMMARY OF RESULTS

The theoretical critical-speed analysis of rigid rotors on flexible foundations yielded these results:

1. Two frequency modes exist. One is the bouncing mode, which is a function of foundation-to-rotor mass and spring-constant ratios only. Another is the conical mode, which is a function of moment-of-inertia and spring-constant ratios as well as rotor rotational speed.

2. The bouncing-mode natural-frequency result comprises two unique solutions.

The following results pertain to the conical-mode natural-frequency and critical-speed solutions.

3. Four unique solutions result that are part of low-frequency and high-frequency two-branch sets of curves. Forward and backward precession are represented by a branch in each set.

4. Although a firm-foundation model predicts only two of the four critical-speed solutions predicted by the flexible-foundation model, its two existing solutions agree well with their flexible-foundation counterparts. The two omitted critical-speed solutions can be approximated by using plus and minus the firm-foundation bouncing-mode solution ($\pi_1 = \pm 1$).

5. At the foundation-to-rotor spring-constant ratio extremities of zero and infinity, the general solution can be approximated by a single two-branch set that represents all geometries. This set is identical to the results given by a firm-foundation model.

6. Because of the existence of this set, only three calculated points are required to

cover the entire range of foundation-to-rotor spring-constant ratio for a specified geometry.

7. The frequency magnitude of forward precession exceeds that of backward precession at all speeds for all rotor shapes.

8. Individually, increasing rotor rotational speed and rotor polar-to-diametral moment-of-inertia ratio each is associated with increased forward-precession and decreased backward-precession frequencies.

9. All frequencies are inversely proportional to $\sqrt{I_1/Ml^2}$.

10. Increase in all frequencies is associated with decreased foundation-to-rotor moment-of-inertia ratio and increased spring-constant ratio.

11. No forward-precession high-frequency critical speeds exist for geometries in which the rotor polar-to-diametral moment-of-inertia ratio equals or exceeds the critical-speed ratio.

12. In backward precession, disks have lower critical speeds than pencil-shape rotors.

13. In summed and differential harmonic oscillation, the number of nonsynchronous critical speeds varies from 3 for a disk to 6 for pencil-shape rotors.

Lewis Research Center,
National Aeronautics and Space Administration,
Cleveland, Ohio, June 12, 1968,
122-29-02-20-22.

REFERENCES

1. Cavicchi, Richard H.: Critical-Speed Analysis of Flexibly Mounted Rigid Rotors. NASA TN D-4607, 1968.

2. Crook, A. W.; and Grantham, F.: An Approach to the Prediction of the Vibrations of Turbine Generators on Undertuned Foundations. Paper No. 67-VIBR-46, ASME, Mar. 29-31, 1967.

3. Gunter, Edgar J., Jr.: Dynamic Stability of Rotor-Bearing Systems. NASA SP-113, 1966.

4. Den Hartog, Jacob Pieter: Mechanical Vibrations. Fourth ed., McGraw-Hill Book Co., Inc., 1956.

5. Timoshenko, Stephen; and Young, Dana H.: Vibration Problems in Engineering. Third ed., D. Van Nostrand Co., Inc., 1955. (Repr. 1966.)

6. Yamamoto, Toshio: On the Critical Speeds of a Shaft. Memoirs of the Faculty of Eng., Nagoya Univ., vol. 6, no. 2, Nov. 1954, pp. 106-174.

7. Yamamoto, Toshio: On Critical Speeds of a Shaft Supported by a Ball Bearing. J. Appl. Mech., vol. 26, no. 2, June 1959, pp. 199-204.

8. Yamamoto, Toshio: On the Vibrations of a Rotating Shaft. Memoirs of the Faculty of Eng., Nagoya Univ., vol. 9, no. 1, May 1957, pp. 19-115.

9. Yamamoto, Toshio; and Hayashi, Satoru: Summed and Differential Harmonic Oscillations in Nonlinear Vibratory Systems. Memoirs of the Faculty of Eng., Nagoya Univ., vol. 18, Nov. 1966, pp. 85-150.

NASA-Langley, 1968 —— 32 E-4375

NATIONAL AERONAUTICS AND SPACE ADMINISTRATION
WASHINGTON, D. C. 20546

OFFICIAL BUSINESS

FIRST CLASS MAIL

POSTAGE AND FEES PAID
NATIONAL AERONAUTICS AND
SPACE ADMINISTRATION

POSTMASTER: If Undeliverable (Section 158 Postal Manual) Do Not Return

"The aeronautical and space activities of the United States shall be conducted so as to contribute . . . to the expansion of human knowledge of phenomena in the atmosphere and space. The Administration shall provide for the widest practicable and appropriate dissemination of information concerning its activities and the results thereof."

—NATIONAL AERONAUTICS AND SPACE ACT OF 1958

NASA SCIENTIFIC AND TECHNICAL PUBLICATIONS

TECHNICAL REPORTS: Scientific and technical information considered important, complete, and a lasting contribution to existing knowledge.

TECHNICAL NOTES: Information less broad in scope but nevertheless of importance as a contribution to existing knowledge.

TECHNICAL MEMORANDUMS: Information receiving limited distribution because of preliminary data, security classification, or other reasons.

CONTRACTOR REPORTS: Scientific and technical information generated under a NASA contract or grant and considered an important contribution to existing knowledge.

TECHNICAL TRANSLATIONS: Information published in a foreign language considered to merit NASA distribution in English.

SPECIAL PUBLICATIONS: Information derived from or of value to NASA activities. Publications include conference proceedings, monographs, data compilations, handbooks, sourcebooks, and special bibliographies.

TECHNOLOGY UTILIZATION PUBLICATIONS: Information on technology used by NASA that may be of particular interest in commercial and other non-aerospace applications. Publications include Tech Briefs, Technology Utilization Reports and Notes, and Technology Surveys.

Details on the availability of these publications may be obtained from:

SCIENTIFIC AND TECHNICAL INFORMATION DIVISION

NATIONAL AERONAUTICS AND SPACE ADMINISTRATION

Washington, D.C. 20546